Thiazolidinedione insulin sensitizers alter lipid bilayer properties and voltage-dependent sodium channel function: implications for drug discovery

Radda Rusinova,[1] Karl F. Herold,[2,5] R. Lea Sanford,[1] Denise V. Greathouse,[4] Hugh C. Hemmings Jr.,[2,3] and Olaf S. Andersen[1]

[1]Department of Physiology and Biophysics, [2]Department of Anesthesiology, and [3]Department of Pharmacology, Weill Cornell Medical College, New York, NY 10065
[4]Department of Chemistry and Biochemistry, University of Arkansas, Fayetteville, AR 72701
[5]Department of Anesthesiology and Intensive Care Medicine, Campus Charité Mitte, 10117 Berlin, Germany

The thiazolidinediones (TZDs) are used in the treatment of diabetes mellitus type 2. Their canonical effects are mediated by activation of the peroxisome proliferator–activated receptor γ (PPARγ) transcription factor. In addition to effects mediated by gene activation, the TZDs cause acute, transcription-independent changes in various membrane transport processes, including glucose transport, and they alter the function of a diverse group of membrane proteins, including ion channels. The basis for these off-target effects is unknown, but the TZDs are hydrophobic/amphiphilic and adsorb to the bilayer–water interface, which will alter bilayer properties, meaning that the TZDs may alter membrane protein function by bilayer-mediated mechanisms. We therefore explored whether the TZDs alter lipid bilayer properties sufficiently to be sensed by bilayer-spanning proteins, using gramicidin A (gA) channels as probes. The TZDs altered bilayer elastic properties with potencies that did not correlate with their affinity for PPARγ. At concentrations where they altered gA channel function, they also altered the function of voltage-dependent sodium channels, producing a prepulse-dependent current inhibition and hyperpolarizing shift in the steady-state inactivation curve. The shifts in the inactivation curve produced by the TZDs and other amphiphiles can be superimposed by plotting them as a function of the changes in gA channel lifetimes. The TZDs' partition coefficients into lipid bilayers were measured using isothermal titration calorimetry. The most potent bilayer modifier, troglitazone, alters bilayer properties at clinically relevant free concentrations; the least potent bilayer modifiers, pioglitazone and rosiglitazone, do not. Unlike other TZDs tested, ciglitazone behaves like a hydrophobic anion and alters the gA monomer–dimer equilibrium by more than one mechanism. Our results provide a possible mechanism for some off-target effects of an important group of drugs, and underscore the importance of exploring bilayer effects of candidate drugs early in drug development.

INTRODUCTION

The thiazolidinediones (TZDs; see Fig. 1) are peroxisome proliferator–activated receptor γ (PPARγ) agonists used in the treatment of type 2 diabetes mellitus to improve target cell insulin sensitivity (Hulin et al., 1996). TZDs reduce plasma triglyceride, fatty acid, and insulin levels, increase HDL cholesterol levels, and promote adipocyte differentiation (Hulin et al., 1996; Fujiwara and Horikoshi, 2000; Sarafidis, 2008)—effects that are mediated by PPARγ-regulated gene transcription.

In addition to the PPARγ-dependent effects, TZDs have off-target effects that do not appear to involve changes in gene transcription. These effects include acute changes in cellular glucose uptake, inhibition of L-type voltage-dependent calcium channels, K_{ATP} channels, and voltage-dependent potassium channels, as well as inhibition of bile acid transport (Table I).

Many off-target TZD effects involve membrane proteins, which are sensitive to changes in their membrane environment (Lee, 2004; Andersen and Koeppe, 2007; Marsh, 2008; Lundbæk et al., 2010a), and amphiphiles tend to be potent modifiers of membrane protein function at the concentrations where they alter lipid bilayer properties (Hwang et al., 2003; Lundbæk et al., 2004, 2005, 2010a; Artigas et al., 2006; Søgaard et al., 2006; Bruno et al., 2007; Ingólfsson et al., 2007). Because the TZDs are amphiphiles, we explored whether they alter lipid bilayer properties and thereby could modulate membrane protein function.

The "nonspecific" regulation of membrane protein function by amphiphiles occurs because of the hydrophobic

R. Rusinova and K.F. Herold contributed equally to this paper.
Correspondence to Radda Rusinova: rar2021@med.cornell.edu

Abbreviations used in this paper: ANTS, 8-aminonaphthalene-1,3,6-trisulfonate; gA, gramicidin A; Na_V voltage-dependent sodium channel(s); PPARγ, peroxisome proliferator–activated receptor γ; SEC, size-exclusion chromatography; TZD, thiazolidinedione.

The Rockefeller University Press $30.00
J. Gen. Physiol. Vol. 138 No. 2 249–270
www.jgp.org/cgi/doi/10.1085/jgp.201010529

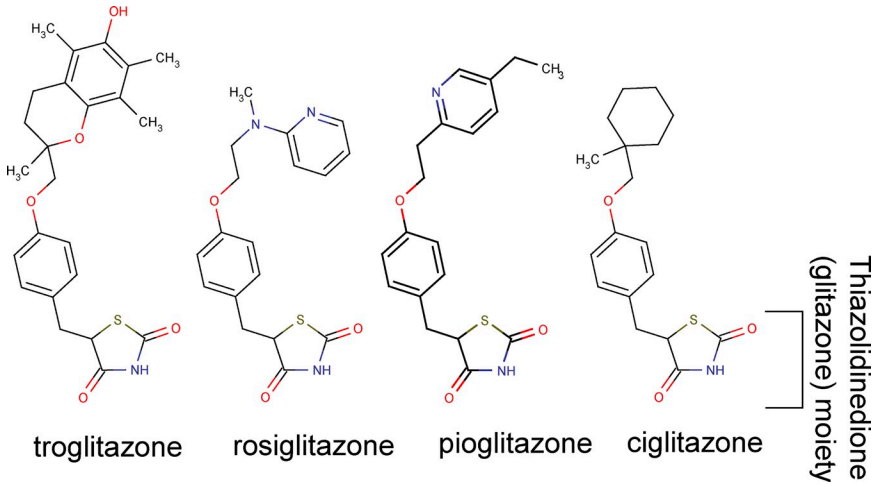

Figure 1. TZD structures. The TZDs are hydrophobic, with octanol–water clogP values (calculated from the experimental $logD_{7.4}$) and $logD_{7.4}$ (experimental) of: 5.3 and 4.2 for troglitazone, 2.8 and 2.6 for rosiglitazone, 3.3 and 3.1 for pioglitazone, and 5.7 and 4.6 for ciglitazone (Giaginis et al., 2007). Calculated pK_a is 6.4 (±0.5) for all of the TZDs (Giaginis et al., 2007). Structures were drawn using MarvinSketch 5.0.3 (ChemAxon).

and energetic coupling between bilayer-spanning proteins and their host lipid bilayer (Fig. 2 A).

The insertion of a protein into a lipid bilayer will locally perturb the bilayer organization to deform the bilayer, which incurs an energetic penalty (the bilayer deformation energy, ΔG_{def}). The difference in bilayer deformation energy between different conformations (denoted I and II) is the bilayer contribution ($\Delta G_{bil}^{I\to II}$) to the free energy difference between I and II:

$$\Delta G_{tot}^{I\to II} = \Delta G_{prot}^{I\to II} + (\Delta G_{def}^{II} - \Delta G_{def}^{I}) = \Delta G_{prot}^{I\to II} + \Delta G_{bil}^{I\to II}. \quad (1)$$

Because ΔG_{def}, and thus $\Delta G_{bil}^{I\to II}$, varies as a function of the bilayer physical properties (thickness, intrinsic monolayer curvature, and the associated elastic moduli), the protein's conformational equilibrium will vary as a function of changes in the host bilayer properties (e.g., Lundbæk and Andersen, 1994; Ashrafuzzaman et al., 2006; Lundbæk et al., 2010a):

$$\frac{n_{II}}{n_I} = K^{I\to II} = \exp\left\{-\frac{\Delta G_{tot}^{I\to II}}{k_B T}\right\} = \exp\left\{-\frac{\Delta G_{prot}^{I\to II} + \Delta G_{bil}^{I\to II}}{k_B T}\right\}, \quad (2)$$

where n_I and n_{II} denote the surface densities of the proteins in state I and II, $K^{I\to II}$ is the equilibrium constant for the I↔II equilibrium, k_B is Boltzmann's constant, and T is the temperature in Kelvin.

When amphiphiles adsorb at the bilayer–solution interface, they alter many bilayer properties, including the intrinsic monolayer curvature (Seddon, 1990; Lundbæk et al., 2005) and bilayer elastic moduli (Evans et al., 1995; Zhelev, 1998), which will alter ΔG_{def} (Fig. 2 B).

TABLE I

Membrane proteins that are modified by the TZDs

TZD	PPARγ EC_{50}[a]	Off-target and effect	EC_{50}[b]	Reference
	μM		*μM*	
Troglitazone	0.5	ATP-sensitive potassium channel K_{ATP}	0.7	Lee et al., 1996
		L-type calcium channels	3–4	Nakamura et al., 1998
		Ca^{2+}-activated potassium channel BK_{Ca}	20–30[c]	Knock et al., 1999; Stowers et al., 2000
		Delayed rectifier potassium channel Kv1.3	3	Ahn et al., 2007
		Acute glucose transport	3[c]	Preininger et al., 1999
		Na^+/H^+ exchange	10[c]	de Dios et al., 2001
		Bile transport (bile salt export pump)	4	Funk et al., 2001;
			10[c]	Snow and Moseley, 2007
Rosiglitazone	0.06–0.09	Voltage-dependent Ca^{2+} current	2[c]	Knock et al., 1999
		Ca^{2+}-activated potassium channels, BK_{Ca}	20[c]	Knock et al., 1999; Stowers et al., 2000
		Delayed rectifier potassium channel Kv1.3	18	Ahn et al., 2007
		Bile transport	10[c]	Snow and Moseley, 2007
Pioglitazone	0.6	L-type calcium channels	45	Nakamura et al., 1998
Ciglitazone	3–23	Ca^{2+}-activated potassium channel BK_{Ca}	16	Stowers et al., 2000
		Store-operated calcium$^+$ channels	30[c]	Kim et al., 2005; Epshtein et al., 2009
		Bile transport	5[c]	Snow and Moseley, 2007

[a]Henke et al., 1998.
[b]Nominal concentrations, not accounting for drug distribution.
[c]Effective concentration.

Changes in bilayer properties will alter membrane protein function when $|\Delta G_{bil}^{I\to II}|$ is a significant ($>k_BT$) contribution to $\Delta G_{tot}^{I\to II}$, in which case changes in $\Delta G_{bil}^{I\to II}$ will alter the energetics and kinetics of the I↔II equilibrium. This may provide a mechanistic basis for the widely observed "membrane effects" of many drugs (Seeman, 1972), including the TZDs.

To explore whether the TZDs alter lipid bilayer properties, we used the gramicidin A (gA) channels as probes (Andersen et al., 2007; Lundbæk et al., 2010a). gA channels are dimers (Bamberg and Läuger, 1973; Veatch et al., 1975), which form by the transmembrane dimerization of nonconducting single-stranded $\beta^{6.3}$-helical subunits that reside in each bilayer leaflet (O'Connell et al., 1990). The kinetics of gA channel formation and disappearance is described by Bamberg and Läuger (1973), Zingsheim and Neher (1974), and Rokitskaya et al. (1996):

$$M+M \underset{k_{-1}}{\overset{k_1}{\rightleftharpoons}} D,$$

where M and D denote monomeric gA subunits (one in each bilayer leaflet) and bilayer-spanning dimers/conducting channels, and k_1 and k_{-1} are the association and dissociation rate constants, with the channel dimerization constant (K_D) given by k_1/k_{-1}. Within wide limits, the gA channel structure is remarkably unaffected by changes in bilayer environment, but the channel lifetime and appearance frequency vary with changes in bilayer thickness, elasticity, and lipid intrinsic curvature (Lundbæk et al., 2010a). The channel function's sensitivity to changes in bilayer properties arises because the channel's hydrophobic length is less than the host bilayer's hydrophobic thickness, such that channel formation produces a local bilayer deformation with an associated deformation energy (Fig. 2 C). In response to the deformation and associated ΔG_{def}, the bilayer exerts a disjoining

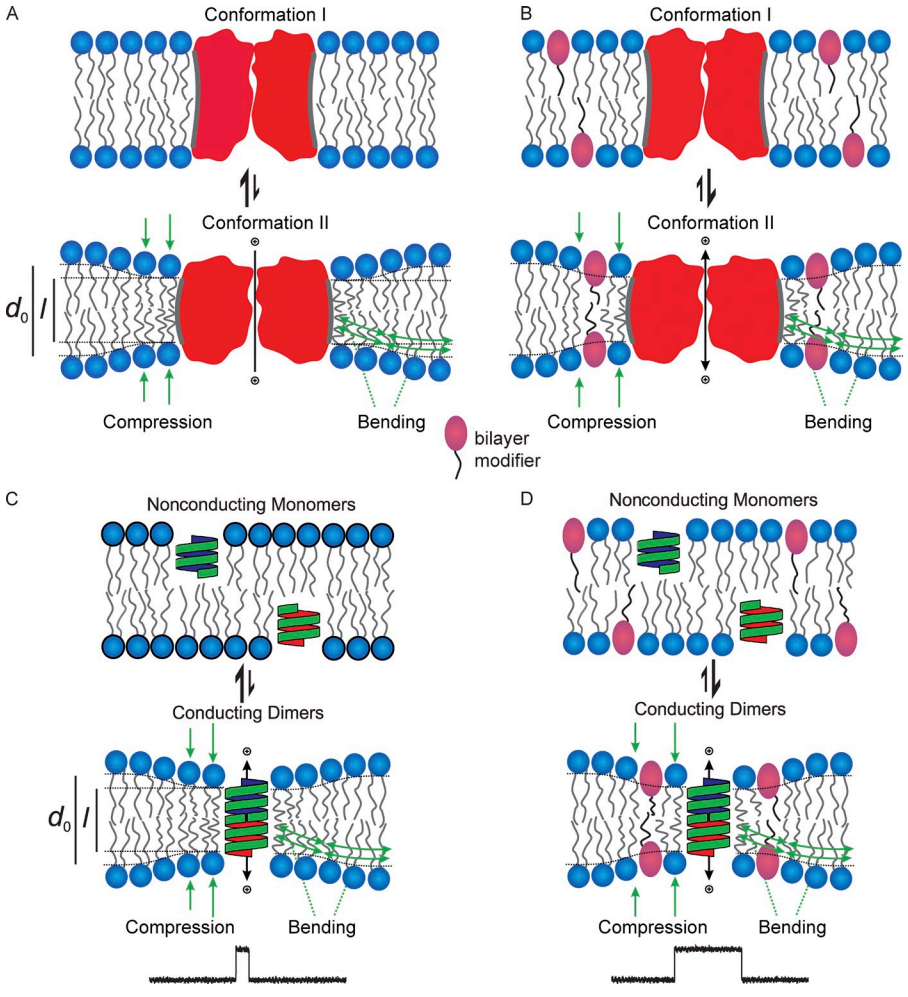

Figure 2. Membrane protein–lipid bilayer hydrophobic coupling. (A) Hydrophobic interactions between integral membrane proteins and their host bilayer cause the lipid bilayer (with an unperturbed hydrophobic thickness d_0) and an embedded protein (with hydrophobic length l) to adapt to each other. Protein conformational changes that involve the protein–bilayer boundary, for example, a change in protein hydrophobic length, will alter the local bilayer thickness to match the channel length. Such local bilayer deformations, with their associated bilayer compression and monolayer bending, incur an energetic cost (the bilayer deformation energy, ΔG_{def}). The total free energy difference between different protein conformations ($\Delta G_{tot}^{I\to II} = \Delta G_{tot}^{II} - \Delta G_{tot}^{I}$) therefore has a contribution not only from the protein per se ($\Delta G_{prot}^{I\to II} = \Delta G_{prot}^{II} - \Delta G_{prot}^{I}$) but also from the difference in bilayer deformation energy associated with the two conformations ($\Delta G_{bil}^{I\to II} = \Delta G_{def}^{II} - \Delta G_{def}^{I}$). The protein conformational equilibrium therefore varies as a function of the bilayer elastic moduli, protein–bilayer hydrophobic mismatch, and the intrinsic lipid curvature. (B) When amphiphiles adsorb to the bilayer–solution interface, they alter bilayer properties such as thickness (d_0), intrinsic curvature (c_0), and elastic moduli, as well as ΔG_{def}. The associated changes in $\Delta G_{bil}^{I\to II}$ will alter the conformational preference and thus its function. (C) Bilayer-spanning gA channels form by transmembrane dimerization of two $\beta^{6.3}$-helical subunits; channel formation is reported as changes in the current through the bilayer. The channel length is less than the unperturbed bilayer thickness, meaning that the energetic cost of channel formation—and the single-channel appearance frequency and lifetime—varies with changes in lipid bilayer properties. (D) Changes in lipid bilayer properties, such as those caused by the adsorption at the bilayer–solution interface, therefore will be reflected in changes in gA lifetimes and appearance frequencies, as indicated in the current trace.

force (F_{dis}) on the dimer, and the rate constant for dimer dissociation varies with changes in F_{dis} (e.g., Lundbæk et al., 2010a). The adsorption of amphiphiles at the bilayer–solution interface alters lipid bilayer elastic moduli and the monolayer-intrinsic curvature, which in turn alters F_{dis}. These changes are observed as increased or decreased gramicidin channel lifetimes and appearance frequencies (Fig. 2 D).

The TZDs alter lipid bilayer properties, with a rank order consistent with previous reports showing troglitazone as the most potent inhibitor of ion channel function (Knock et al., 1999; Ahn et al., 2007). They also inhibit voltage-dependent sodium channels (Na_V). Similar to other amphiphiles (Lundbæk et al., 2005), the TZDs cause a hyperpolarizing shift in the steady-state availability curve. The concentration dependence of the TZDs' effects on Na_V is similar to that for gA channels, and the correlation between the TZD effects on gA and Na_V channels can be superimposed on the relation observed for other amphiphiles (Lundbæk et al., 2005), suggesting that some TZD off-target effects are mediated by changes in bilayer properties.

MATERIALS AND METHODS

Gramicidin experiments

Materials. 1,2-dioleoyl-*sn*-glycero-3-phosphocholine ($DC_{18:1}PC$), 1,2-dieicosenoyl-*sn*-glycero-3-phosphocholine ($DC_{20:1}PC$), 1,2-dierucoyl-*sn*-glycero-3-phosphocholine ($DC_{22:1}PC$), and cholesterol were from Avanti Polar Lipids, Inc. *n*-Decane (99.9% pure) was from ChemSampCo. Troglitazone, rosiglitazone, and ciglitazone (≥98% purity) were from Cayman Chemical. Pioglitazone (≥99.3% purity) was from Tecoland Corporation. 8-Aminonaphthalene-1,3,6-trisulfonate (ANTS) was from Invitrogen. A chain-shortened 13–amino acid left-handed gA analogue, des-D-Val-Gly-gA^- ($gA^-(13)$), two 15–amino acid analogues of opposite helix sense, [Ala^1]gA (AgA(15)) and [D-Ala^1]gA^- ($AgA^-(15)$), and a chain-extended 17–amino acid analogue, endo-Ala^{0a}-D-Ala^{0b}-gA (gA(17)), were synthesized and purified as described previously (Greathouse et al., 1999). Their sequences are listed in Table S1.

Single-channel current measurements. Planar lipid bilayers were formed at 25 ± 1°C using 20-mg/ml suspensions of $DC_{18:1}PC$, $DC_{18:1}PC$/cholesterol (1:1 molar ratio), or $DC_{20:1}PC$ in *n*-decane across a 1–1.5-mm opening in a Teflon partition separating two 2.5-ml compartments. The chamber and electrode solutions were 1.0 M NaCl and 10 mM HEPES, pH 7. Single-channel measurements were done at ±200 mV using a patch-clamp amplifier (3900A; Dagan Corp.) and the bilayer punch method (Andersen, 1983; Kapoor et al., 2008). The current signal was filtered at 2 kHz, sampled at 20 kHz, and digitally filtered at 500 Hz. Single-channel current transitions were identified as described previously (Andersen, 1983) using software written in Visual Basic (Microsoft). The gA analogues were added to both sides of the bilayer. In most experiments, we used two analogues of different length and helix sense, which allowed us to explore the role of hydrophobic mismatch. After control records were obtained, we added TZD from stock solutions (prepared in DMSO) to each side of the bilayer, stirred for 1 min, and equilibrated for 10 min. The DMSO concentration never exceeded 0.7% (vol/vol), which by itself has no effect on bilayer properties (Ingólfsson and Andersen, 2010).

Single-channel lifetimes (τ) were determined by fitting a single-exponential distribution ($N(t)/N(0) = \exp\{-t/\tau\}$, where $N(t)$ is the number of channels with lifetimes longer than time, t, to the survivor histograms of the lifetime distributions using Origin 6.1 (OriginLab). The reported results are the averages of three to five experiments, each with at least 300 events. Changes in channel appearance frequency (f) are based on single-channel recordings (>5 min) immediately before and immediately after adding the TZDs. Only experiments where the bilayer remained intact after TZD addition were used. The results are reported as mean ± SD; in case there are only two observations, the results are reported as mean ± range. Relative lifetime and appearance frequency changes were obtained by normalizing the values just after to those just before adding the TZD.

From the changes in the time-averaged channel density ($= f\cdot\tau$) one can calculate the changes in the channel dimerization constant (K_D) as (Hwang et al., 2003):

$$\frac{f_{TZD}\cdot\tau_{TZD}}{f_{cntrl}\cdot\tau_{cntrl}} = \frac{[D]_{TZD}}{[D]_{cntrl}} = \frac{k_{1,TZD}\cdot[M]^2_{TZD}/k_{-1,TZD}}{k_{1,cntrl}\cdot[M]^2_{cntrl}/k_{-1,cntrl}} = \frac{K_{D,TZD}}{K_{D,cntrl}}, \quad (3)$$

where the subscripts "cntrl" and "TZD" indicate the absence and presence of the TZD, and the third equality holds in the limit $[M] \gg [D]$ (when [M] is approximately constant). One can then calculate the changes in the free energy of dimerization ($\Delta\Delta G^{M\to D}_{tot}$) and, if the TZDs do not alter $\Delta G^{M\to D}_{prot}$, the changes in $\Delta G^{M\to D}_{bil}$, cf. Eq. 1:

$$\Delta\Delta G^{M\to D}_{tot} = -k_BT\cdot\ln\left\{\frac{K_{D,TZD}}{K_{D,cntrl}}\right\} \approx -k_BT\cdot\ln\left\{\frac{f_{TZD}\cdot\tau_{TZD}}{f_{cntrl}\cdot\tau_{cntrl}}\right\} \approx \Delta\Delta G^{M\to D}_{bil}, \quad (4)$$

where the right-most relation holds when $\Delta\Delta G^{M\to D}_{prot} \approx 0$.

The capacitance of $DC_{18:1}PC$ bilayers (area, ~1.5 mm^2) was measured using the current response to a 2.5-Hz saw tooth potential of 10-mV peak-to-peak amplitude (Lundbæk et al., 1996).

Fluorescence quench measurements. This method has been described elsewhere (Ingólfsson and Andersen, 2010; Ingólfsson et al., 2010). In brief, $DC_{22:1}PC$ in chloroform was dried and rehydrated in fluorophore (ANTS) buffer. Large unilamellar vesicles were prepared by passing the rehydrated lipid suspension through 0.1-µm membrane using a mini-extruder (Avanti Polar Lipids, Inc.), and extravesicular ANTS was removed using a desalting column (PD-10; GE Healthcare). ANTS-loaded vesicles were incubated with gA for 24 h at 12°C. The rate of ANTS fluorescence quenching by the gA channel–permeant Tl^+ was recorded with a stopped-flow spectrofluorometer (SX.20; Applied Photophysics) with dead time of <2 ms. Samples were excited at 352 nm, and the fluorescence signal above 455 nm was recorded. Vesicles were incubated with the TZD for 10 min at 25°C before measuring the quenching rate. TZDs are hydrophobic and cross the cell membrane to reach PPARγ; they likewise will equilibrate between the inner and the outer bilayer leaflets. Nine mixing reactions were done with each sample. Each reaction was analyzed separately using MATLAB v7.9 (The MathWorks Inc.). Quenching rates were determined by fitting the first 2–100 ms of the fluorescence time course for the individual reactions with stretched exponential (Berberan-Santos et al., 2005):

$$F(t) = F(\infty) + \big(F(0) - F(\infty)\big)\cdot\exp\left\{-(t/\tau_0)^\beta\right\}, \quad (5)$$

where $F(t)$ denotes the fluorescence intensity as a function of time, t, τ_0 is a parameter with units of time, and β ($0 < \beta \le 1$) is a measure of the dispersity of the sample. We then determined the

quenching rate at 2 ms using the expression (Berberan-Santos et al., 2005):

$$k(t) = (\beta / \tau_0) \cdot (t / \tau_0)^{(\beta-1)}. \quad (6)$$

The average quenching rate is the average of these rates. The reported values are averages of the quenching rates, normalized to rate in the absence of TZDs, for three or more experiments.

Isothermal titration calorimetry. Heats of adsorption were measured using an isothermal titration calorimeter (Auto-iTC$_{200}$; Microcal Inc.) with 200-µl sample cell volume and 40-µl syringe volume. Large unilamellar DC$_{20:1}$PC or DC$_{18:1}$PC vesicles were prepared as described above, with the following modifications: the lipid rehydration buffer (150 mM $NaNO_3$ and 15 mM HEPES, pH 7) did not contain ANTS, and the vesicles were not incubated with gA. TZDs were diluted from DMSO stocks with the lipid rehydration buffer. The DMSO concentration in the lipid vesicle solution was adjusted to match the TZD-containing solution.

The lipid vesicle solution was in the syringe, and the TZD solution was in the sample cell. Titration of lipid vesicles into the TZD solution was done with 2-µl injections (the first 0.2-µl injection was not taken into account during analysis). The 150-s interval between each injection allowed the signal to return to the baseline and was sufficient for equilibration of TZDs between the inner and outer bilayer leaflets. After 19 injections of 3 mM lipid into 30 µM troglitazone, or 10 mM lipid into 200 µM rosiglitazone, the lipid concentrations were 460 µM or 1.5 mM, respectively; all the TZD was considered to be bound to the lipid vesicles when the heat generation in subsequent injections became constant. (Ciglitazone and pioglitazone did not produce a measurable signal.) To control for heat of dilution of buffer and lipid vesicles, lipid vesicles were injected into a TZD-free buffer solution. The resulting enthalpies were below the detection limit of the instrument (Fig. S9); we did not correct for them in the data analysis. The enthalpy per injection was determined from the area under the curve of that injection using Origin 7 (OriginLab) as adapted by Microcal for isothermal titration calorimetry data analysis. The partition constant $K_P^{W\to L}$ and enthalpy of partitioning $\Delta H_P^{W\to L}$ were obtained by plotting the injection enthalpies versus injection number and fitting using Eq. 7 (derived according to Wenk et al., 1997), assuming that the process can be described as partitioning between two immiscible phases (cf., White et al., 1998):

$$\begin{aligned}\delta h_A(i) &= \frac{i\cdot\delta V\cdot C_L\cdot v_L\cdot n_{tot}^A\cdot\Delta H_P^{W\to L}\cdot K_P^{W\to L}}{V_W(0)+i\cdot\delta V\cdot\left(1+C_L\cdot v_L\cdot K_P^{W\to L}\right)}\\ &\quad-\frac{(i-1)\cdot\delta V\cdot C_L\cdot v_L\cdot n_{tot}^A\cdot\Delta H_P^{W\to L}\cdot K_P^{W\to L}}{V_W(0)+(i-1)\cdot\delta V\cdot\left(1+C_L\cdot v_L\cdot K_P^{W\to L}\right)}\\ &\approx\frac{\delta V\cdot C_L\cdot v_L\cdot n_{tot}^A\cdot V_W(0)\cdot\Delta H_P^{W\to L}\cdot K_P^{W\to L}}{\left(V_W(0)+(i-0.5)\cdot\delta V\cdot\left(1+C_L\cdot v_L\cdot K_P^{W\to L}\right)\right)^2},\end{aligned} \quad (7)$$

where i is the injection number, $\delta h_A(i)$ the injection enthalpy, δV is the injection volume, C_L is the lipid concentration, v_L is the molar lipid volume, n_{tot}^A is the amount of amphiphile in moles, and $V_W(0)$ is the initial cell volume. Knowing $K_P^{W\to L}$ and $\Delta H_P^{W\to L}$ (assuming ΔH_P is measurable), the free energy ($\Delta G_P^{W\to L}$) and entropy ($\Delta S_P^{W\to L}$) of partitioning is calculated as $\Delta G_P^{W\to L} = \Delta H_P^{W\to L} + T\cdot\Delta S_P^{W\to L}$, where $\Delta G_P^{W\to L} = -RT\ln(K_P^{W\to L})$.

Sodium channel current measurements

Cell culture. The ND7/23 rat dorsal root ganglion/mouse neuroblastoma fusion cell line (Sigma-Aldrich) was cultured in Dulbecco's modified Eagle's medium (Invitrogen) supplemented with 10% (vol/vol) fetal bovine serum (Invitrogen), 2 mM L-glutamine, 100 U/ml penicillin, and 100 µg/ml streptomycin (Invitrogen) at 37°C under 95% air/5% CO_2. Cells were grown on 12-mm glass coverslips in 35-mm polystyrene culture dishes and used within 48–72 h of plating.

Electrophysiology. Endogenous TTX-sensitive Na^+ currents (ND7/23 cells express a combination of Na_V subtypes 1.1, 1.2, 1.6, and 1.7, as shown by Western blotting; not depicted) were recorded using the whole cell clamp configuration (Hamill et al., 1981). Coverslips containing ND7/23 cells were transferred into a small-volume open bath chamber (Warner Instruments) and continuously perfused at ~2 ml/min with a solution containing (in mM): 130 NaCl, 10 HEPES, 3.25 KCl, 2 $MgCl_2$, 2 $CaCl_2$, 20 TEACl, and 5 D-glucose, adjusted to pH 7.4 (with NaOH), and 310 mOsm/kg H_2O (with sucrose).

Voltage-clamp recordings were done at room temperature (23–24°C) using a patch-clamp amplifier (Axopatch 200B; Molecular Devices) with a sampling rate of 20- and 5-kHz low-pass filter. Recording pipettes were pulled from borosilicate glass capillaries (Sutter Instrument) on a puller (P-97; Sutter Instruments) and fire-polished. The pipettes were filled with a solution containing (in mM): 120 CsF, 10 NaCl, 10 HEPES, 10 EGTA, 10 TEACl, 1 $CaCl_2$, and 1 $MgCl_2$, adjusted to pH 7.3 (with CsOH), and 310 mOsm/kg H_2O (with sucrose). The pipettes had a tip resistance of 1.5–2.5 MΩ. The access resistance, 2–4 MΩ, was further decreased using 70–80% series resistance compensation. The initial whole cell seal resistance was 2–4 GΩ, and recordings were discarded if the resistance dropped below 1 GΩ. Liquid–junction potentials were not corrected. Capacitive current transients were electronically cancelled with the internal amplifier circuitry, and leak currents were digitally subtracted online using the P/4 protocol (Bezanilla and Armstrong, 1977).

The TZDs dissolved in DMSO were diluted in the external perfusion buffer to their final concentration before experiments the same day. Final DMSO concentrations did not exceed 0.7% (vol/vol). (1% DMSO has no effect on activation or inactivation; not depicted.) The perfusion system consisted of Teflon tubing connected to a 200-µm diameter perfusion pipette positioned in close proximity to the patch-clamped cell. The perfusion rate was ~0.2 ml/min and controlled by a pressurized perfusion system (ALA Scientific Instruments).

Stimulation protocols and data analysis. The holding potential (V_h) was −80 mV unless otherwise stated. Voltage-dependent inhibition of peak inward Na^+ current (I_{Na}) by TZDs was analyzed using a 10-ms test pulse to 0 mV preceded by a 300-ms prepulse alternating to either −130 mV (V_0) or the voltage of half-maximal inactivation ($V_{1/2} = -68 \pm 5$ mV), applied every 5 s (Lundbæk et al., 2004). $V_{1/2}$ was determined for each cell using the two-pulse protocol described below.

For examining Na^+ channel activation, currents were evoked by a series of 10-ms pulses ranging from −60 to +70 mV in 10-mV steps every 5 s. The conductance (G_{Na}) was calculated as $G_{Na} = I_{Na}/(V_m - E_{rev})$, where I_{Na} is the peak inward current, V_m is the amplitude of the voltage step, and E_{rev} is the reversal potential (about +65 mV), as estimated using the Nernst equation and the internal and external Na^+ concentrations of 10 and 130 mM, respectively; the recorded E_{rev} varied between 65 and 68 mV and did not change with TZD application (not depicted). The normalized conductance (G/G_{max}, where G_{max} is the maximal conductance) was plotted versus V_m and fitted with a Boltzmann function:

$$G/G_{max} = 1/\left(1+\exp\{-e\cdot z_a\cdot(V_m - V_a)/k_BT\}\right), \quad (8)$$

where V_a is the potential for half-maximal activation, e is the elementary charge, and z_a is the apparent gating valence.

Steady-state fast inactivation, or "Na^+ channel availability," h_∞ in Hodgkin and Huxley (1952), was measured using a double-pulse protocol with a 300-ms prepulse ranging from −130 to −10 mV in 10-mV steps, followed by a test pulse to 0 mV. Peak currents during the test pulse were normalized to the maximal current (I/I_{max}, where I_{max} is the maximal current that is elicited at the test potential), plotted versus the prepulse potential (V_m), and fitted with a Boltzmann function:

$$I / I_{max} = 1 / \left(1 + \exp\left\{-e \cdot z_{1/2} \cdot (V_m - V_{1/2}) / k_B T\right\}\right), \quad (9)$$

where $z_{1/2}$ and $V_{1/2}$ denote the apparent gating valence and potential for half-maximal inactivation.

Statistical significance was assessed by two-tailed paired Student's t test. $P < 0.05$ was considered statistically significant. Programs used for data acquisition and analysis were pClamp 10 (Molecular Devices), Excel (Microsoft), and Prism 5.0 (GraphPad Software Inc.). Values are reported as mean ± SD unless otherwise stated.

Online supplemental material

Fig. S1 shows TZD's effects on gA single-channel currents. Fig. S2 shows ciglitazone's effects on gA single-channel currents at pH 6, 7, and 8. Fig. S3 shows pioglitazone's effects on gA function at pH 6. Fig. S4 shows TZD effects on gA channel lifetimes. Fig. S5 shows changes in $gA^-(13)$ lifetimes relative to changes in AgA(15) lifetimes in the presence of TZDs. Fig. S6 shows relative lifetimes of $gA^-(15)$ and gA(17) in $DC_{20:1}PC$ bilayers as function of [ciglitazone]. Fig. S7 compares the effects of troglitazone and ciglitazone on gA activity in the presence and absence of cholesterol in $DC_{18:1}PC$ bilayers. Fig. S8 shows fluorescence quenching traces from stopped-flow experiments with ciglitazone and troglitazone. Fig. S9 shows dilution enthalpies of lipid in TZD-free buffer solution. Fig. S10 shows timed control experiments for the Na_V inactivation experiments. Fig. S11 shows ciglitazone's effects on gA single-channel currents in $DC_{20:1}PC$ bilayers. Table S1 lists the sequences of the gA analogues used in this study. Table S2 lists the Na_V peak current inhibition, Table S3 lists the $V_{1/2}$ of steady-state inactivation, and Table S4 lists the $V_{1/2}$ of activation before, during, and after TZD superfusion.

RESULTS

Gramicidin experiments

TZDs alter gA channel function. The TZD effects on gA channel function were examined by comparing the gA single-channel properties before and after the addition of each TZD. The left-handed 13–amino acid $gA^-(13)$ and the right-handed 15–amino acid AgA(15) analogues form channels with characteristic current transition amplitudes, marked in Fig. 3 A by red and blue lines for $gA^-(13)$ and AgA(15), respectively. (Because the two analogues form channels having opposite handedness, they do not form heterodimers.) Fig. 3 (A–D) shows single-channel activity before and after the addition of each TZD.

Troglitazone rosiglitazone and pioglitazone increase gA channel activity, the time-averaged number of channels (Fig. 3, A–C); 6 μM ciglitazone decreased the activity of both $gA^-(13)$ and AgA(15) channels (bottom trace in Fig. 3 D). The TZDs are potent modifiers of gA channel function, with effects that vary among the compounds tested.

Changes in gA single-channel properties. The changes in gA channel activity reflect changes in the energetics of

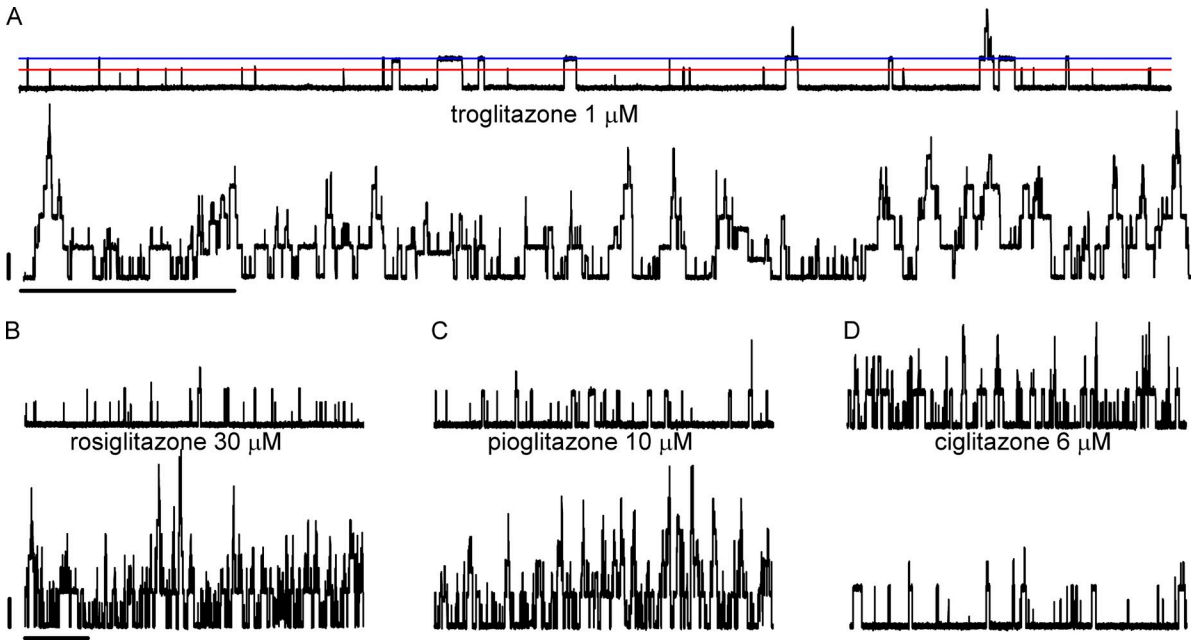

Figure 3. TZD-induced changes in gA function. Current traces before and after the addition of each of the four TZDs to both sides of a $DC_{18:1}PC$/*n*-decane bilayer doped with $gA^-(13)$ and AgA(15). In each panel, the top trace was recorded before adding the TZD, and the bottom trace was recorded after the addition. The colored lines denote the current levels for $gA^-(13)$ (red line) and AgA(15) (blue line). The four panels show the effects of: (A) 1 μM troglitazone, (B) 30 μM rosiglitazone, (C) 10 μM pioglitazone, and (D) 6 μM ciglitazone. Bars, 3 pA and 30 s.

gA channel formation. To characterize these changes, we examined the TZDs' effects on gA single-channel current transition amplitudes, lifetimes, and appearance frequencies. The current transition amplitude histograms (Fig. 4, A and B, and Fig. S1), show that TZDs—except for ciglitazone, which caused a modest increase (Fig. 4 B)—did not alter the conductances of $gA^-(13)$ or AgA(15) channels at the highest concentrations tested. The lack of effect on the gA single-channel conductance suggests that troglitazone, rosiglitazone, and pioglitazone do not bind to, or otherwise interact directly with, gA channels.

The conductance changes caused by ciglitazone could reflect that ciglitazone is a weak acid (pK of ~6.4; Giaginis et al., 2007). Adsorption of the anionic form of ciglitazone at the bilayer/solution would increase the local $[Na^+]$, and thus the single-channel conductance (Apell et al., 1979). If so, the ciglitazone-induced conductance should be pH dependent, which it is; at pH 8, the conductance increase was greater than at pH 7, and at pH 6, there was no conductance increase (Fig. S2). These results suggest that the conductance changes occur because the anionic form of ciglitazone adsorbs at the bilayer–solution interface and effectively excludes that the conductance changes are a result of changes in the interfacial dipole potential. We also examined whether similar pH-dependent conductance changes occurred with pioglitazone. They did not (Fig. S3). We do not understand why only ciglitazone alters the single-channel conductance

Troglitazone increased the lifetimes (τ) of both $gA^-(13)$ and AgA(15) channels with a 50% increase at 1 µM (Figs. 4 C and 5 A). Rosiglitazone caused similar increases in τ, but at 30-fold higher concentrations (Figs. S4 B and 5 B). Pioglitazone did not alter τ at concentrations up to 10 µM, its solubility limit (Figs. S4 C and 5 C). Ciglitazone caused moderate increases in τ at concentrations up to 6 µM, where the effect appears to saturate (Figs. 4 D and 5 D). (The ciglitazone-induced changes in τ did not vary as a function of pH; not depicted.)

Similar to many other amphiphiles (Lundbæk et al., 2005), troglitazone, rosiglitazone, and ciglitazone caused larger relative increases in τ of $gA^-(13)$ as compared with AgA(15) channels (Fig. S5, A, B, and D). We return to this below.

The TZDs also alter the channel appearance frequencies (f) (Fig. 3). The changes in f were evaluated in experiments in which the bilayer did not break during/after the addition of the TZD (Fig. 5, E–H), which limits our ability to explore changes caused by troglitazone and rosiglitazone above 1 and 30 µM, respectively, because bilayers break upon the addition of higher concentrations. 1 µM troglitazone (Fig. 5 E), 30 µM rosiglitazone (Fig. 5 F), and 10 µM pioglitazone (Fig. 5 G) increased f for $gA^-(13)$ and AgA(15) channels, with the larger effect on the shorter $gA^-(13)$ channels. 6 µM ciglitazone reduced f for $gA^-(13)$ channels to ~50% of control with little effect on AgA(15) channels (Fig. 5 H). This effect is, at least in part, dependent on channel–bilayer hydrophobic mismatch, as ciglitazone reduced f for $AgA^-(15)$ channels in $DC_{20:1}PC/n$-decane bilayers (not depicted).

Troglitazone and rosiglitazone had larger effects on f (Fig. 5, E and F) than on τ (Fig. 5, A and B), reflecting the greater sensitivity of the gA dimerization rate constant, as compared with the dissociation rate constant, to changes in bilayer properties (Lundbæk et al., 2005).

The TZDs alter lipid bilayer properties. The results in Figs. 3–5 show that the TZDs alter gA channel function. The TZDs have quantitatively similar effects on left- and

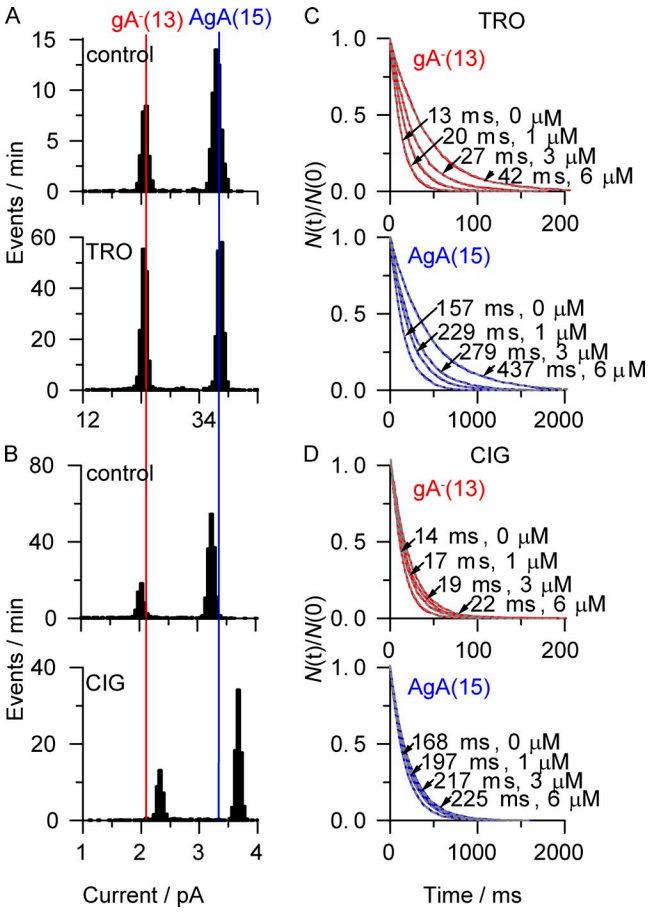

Figure 4. Effects of TZDs on ion permeation and single-channel lifetimes. Current transition amplitude histograms for $gA^-(13)$ and AgA(15) channels before (control) and after the addition of: (A) 6 µM troglitazone (TRO) and (B) 6 µM ciglitazone (CIG). The vertical lines denote the single-channel current transition amplitudes in the absence of the TZD for $gA^-(13)$ (red line) and AgA(15) (blue line). Single-channel survivor histograms for $gA^-(13)$ (red line) and AgA(15) (blue line) channels in the presence of varying concentrations of: (C) troglitazone (TRO) and (D) ciglitazone (CIG). Each plot was fitted with a single-exponential distribution (dashed gray lines); the average lifetimes (τ) for each TZD and concentration are indicated in the panels.

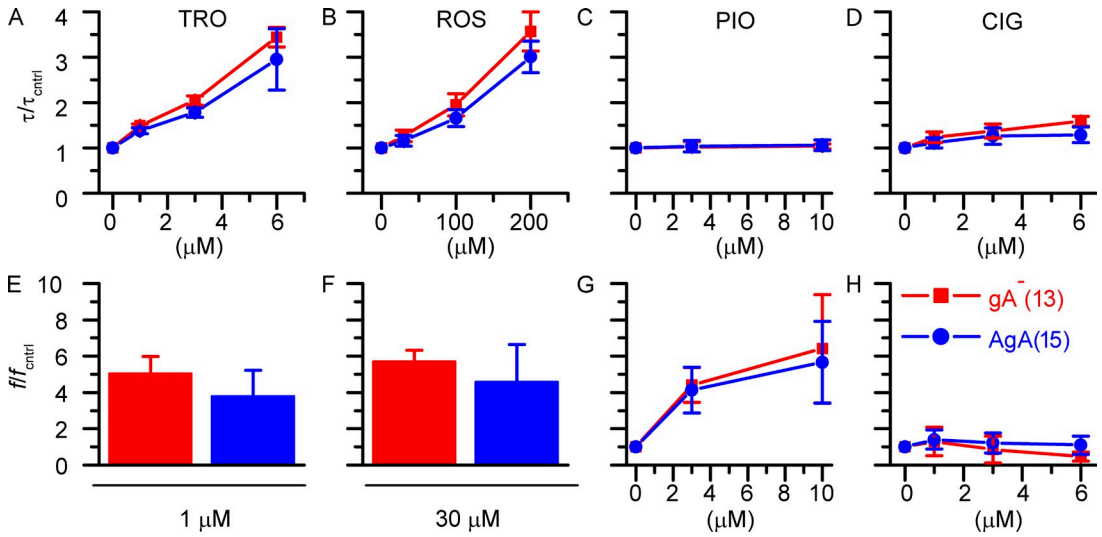

Figure 5. TZD-induced changes in single-channel lifetime and appearance frequency. Relative changes in $gA^-(13)$ (red squares) and AgA(15) (blue circles) channel lifetimes as a function of [TZD], normalized to the lifetimes before TZD addition for: (A) troglitazone (TRO), (B) rosiglitazone (ROS), (C) pioglitazone (PIO), and (D) ciglitazone (CIG; $n = 4–7$). The appearance frequency after is normalized to the appearance frequency before the addition of the TZD: (E) 1 μM troglitazone (TRO), (F) 30 μM rosiglitazone (ROS), (G) pioglitazone (PIO), and (H) ciglitazone (CIG; $n = 2–4$).

right-handed gA channels (Fig. 5), and when plotting $\ln\{\tau/\tau_{cntrl}\}$, where "cntrl" denotes results in the absence of amphiphile, for $gA^-(13)$ channels versus $\ln\{\tau/\tau_{cntrl}\}$ for AgA(15) channels (Fig. 6), the results for the TZDs and structurally unrelated compounds (Lundbæk et al., 2010b) are described by a shared linear relation with a slope of ~1.2. That is, the TZDs conform to the pattern observed with other bilayer-modifying amphiphiles, indicating that all of these compounds alter the lifetimes by a common mechanism.

This commonality shows that these compounds act through a common mechanism and excludes that they alter τ through direct interactions with the bilayer-spanning $\beta^{6.3}$-helical dimers. Because amphiphiles alter lipid bilayer properties, including their elastic moduli (e.g., Evans et al., 1995; Zhelev, 1998; Ly and Longo, 2004; Zhou and Raphael, 2005), the most likely common mechanism is that the TZD, like other amphiphiles, alter gA channel lifetimes by altering lipid bilayer properties.

The situation is more complicated, however. Although the ciglitazone-induced changes in τ are consistent with bilayer-mediated mechanism (Fig. 6), no change in *f* of AgA(15) channels and a decrease in *f* for $gA^-(13)$ channels indicate that this compound has additional effects. The decreased appearance frequency (for the $gA^-(13)$ channels) could reflect a shift in the equilibrium between conducting single-stranded and nonconducting double-stranded dimers (Sychev et al., 1993; Greathouse et al., 1994; Galbraith and Wallace, 1998), or a shift between different monomeric conformers. We explored this using size-exclusion chromatography (SEC) and found no effect on the distribution between single-stranded and double-stranded conformers (Kapoor, R., personal communication). We conclude that ciglitazone does not have specific interactions with the bilayer-spanning single-stranded $\beta^{6.3}$-helical gA dimers. Pioglitazone did not alter τ at the concentrations tested (Fig. 5 C), most likely reflecting its limited solubility and rather low logP, and consequently low membrane concentration. Yet, pioglitazone increases *f* with similar

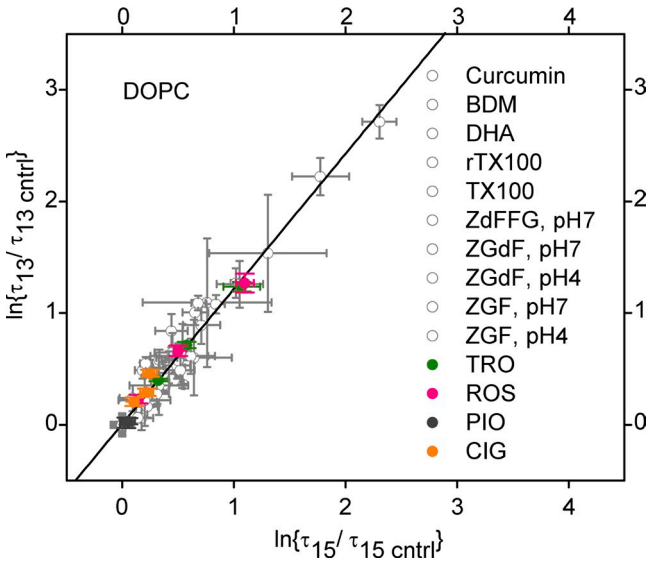

Figure 6. Changes in $gA^-(13)$ channel lifetimes (τ_{13}) as a function of the corresponding changes in AgA(15) channel lifetimes (τ_{15}). Gray data are from Lundbæk et al. (2010b). The colored results are from this study; each point represents the average value from two to seven experiments. Color code: olive, troglitazone (TRO); pink, rosiglitazone (ROS); orange, ciglitazone (CIG); gray, pioglitazone (PIO). Linear fit (solid line) to the data points has a slope of 1.24 ($r = 0.997$).

effects on right- and left-handed channels (Fig. 5 G). We do not understand why, but note that pioglitazone is completely inert in cholesterol-containing bilayers (see below), effectively excluding specific pioglitazone–gA interactions.

The TZDs do not alter bilayer thickness. The TZD-induced changes in gA channel function could result from changes in bilayer thickness. Bilayer thinning will result in capacitance increase $C_m = \varepsilon_0\varepsilon_r / d_0$, where C_m is the specific capacitance of the bilayer, ε_o is the permittivity of free space, ε_r is the relative dielectric constant, and d_0 is the bilayer hydrophobic thickness. We determined the TZDs' effects on C_m of $DC_{18:1}PC$ bilayers. Troglitazone (mean ± SD: control, 4.8 ± 0.3 nF/mm^2; 10 μM troglitazone, 4.9 ± 0.2 nF/mm^2), rosiglitazone (control, 4.8 ± 0.2 nF/mm^2; 100 μM rosiglitazone, 4.7 ± 0.3 nF/mm^2), and pioglitazone (control, 4.9 ± 0.1 nF/mm^2; 10 μM pioglitazone, 4.9 ± 0.1 nF/mm^2) did not increase C_m, demonstrating that the increases in τ and f do not result from bilayer thinning. 6 μM ciglitazone increased C_m ~16% (C_m ± SD: control, 4.9 ± 0.2 nF/mm^2; 6 μM ciglitazone, 5.7 ± 0.2 nF/mm^2).

The modest ciglitazone-induced increase in τ is not consistent with the bilayer thinning predicted from the capacitance increase. Rather, ciglitazone may act like a hydrophobic anion and increase the membrane capacitance by intramembrane charge transfer (Fernández et al., 1983). Indeed, ciglitazone increases the bilayer conductance. 10 μM ciglitazone increases the steady-state conductance from 10^{-8} S/cm^2 to 4×10^{-8} S/cm^2, consistent with an aqueous diffusion-limited current (Le Blanc, 1969). This effect seems to be specific for ciglitazone; 6 μM troglitazone had no effect on the bilayer conductance.

The TZDs alter the energetics of gA dimerization and lipid bilayer elasticity. To minimize the exposure of hydrophobic residues to water, gA channels and their host bilayer are coupled though hydrophobic interactions, and the formation of gA channels of hydrophobic length (l) in a bilayer of hydrophobic thickness (d_0) causes a local change in bilayer thickness, a thinning because l is less than d_0 (Fig. 2, C and D). Changes in the energetics of the associated bilayer deformation (Huang, 1986; Helfrich and Jakobsson, 1990; Nielsen et al., 1998; Nielsen and Andersen, 2000; Partenskii and Jordan, 2002) will alter the kinetics and energetics of gA channel formation (Lundbæk et al., 2010a).

From the changes in $f (= k_1 \cdot [M]^2)$ and τ $(= 1/k_{-1})$, one can calculate the changes in the time-averaged channel density, K_D (see Materials and methods). Table II summarizes the TZD-induced changes in $f \cdot \tau$ and $\Delta\Delta G_{tot}^{M\to D}$ for troglitazone, rosiglitazone, pioglitazone, and ciglitazone. In the case of troglitazone and rosiglitazone, the TZDs appear to act through a bilayer-mediated mechanism (meaning that $\Delta\Delta G_{prot}^{M\to D} \approx 0$) and $\Delta\Delta G_{bil}^{M\to D} \approx \Delta\Delta G_{tot}^{M\to D}$.

In response to the bilayer deformation and associated $\Delta G_{bil}^{M\to D}$, the bilayer exerts a disjoining force (F_{dis}) on the channels. F_{dis} varies a function of the hydrophobic mismatch ($d_0 - l$), the elastic coefficients H_B and H_X, and the intrinsic monolayer curvature c_0 (see Eq. A5):

$$F_{dis} = 2 \cdot H_B \cdot (d_0 - l) - H_X \cdot c_0. \tag{10}$$

The relative increases in τ for the $gA^-(13)$ channels were larger than for the AgA(15) channels (Figs. S5 A, B, and D, and 6), meaning that the hydrophobic mismatch-dependent term in Eq. 10 contributes to the changes in F_{dis} (and $\Delta G_{bil}^{M\to D}$). Changes in $H_B \cdot (l - d_0)$ could be a result of changes in H_B or d_0 (the gA channel structure, and thus l, is insensitive to changes in bilayer thickness; Wallace et al., 1981; Katsaras et al., 1992). The changes in H_B can be estimated by comparing the relative change in the lifetimes of the longer and shorter channels (Lundbæk et al., 2010a):

$$\frac{\tau_{15}^{cntrl} \cdot \tau_{13}^{TZD}}{\tau_{15}^{TZD} \cdot \tau_{13}^{cntrl}} = \exp\left\{\frac{2 \cdot \delta \cdot (H_B^{TZD} - H_B^{cntrl}) \cdot (l_2 - l_1)}{k_B T}\right\}, \tag{11}$$

where the subscripts 13 and 15 denote the two channel types. Using Eq. 11, we find that 6 μM troglitazone and 200 μM rosiglitazone decrease H_B by ~4 kJ/(mole·nm^2) or ~1.6 k_BT/nm^2; 1 μM troglitazone and 30 μM rosiglitazone decrease H_B by ~1.5 kJ/(mole·nm^2) or ~0.6 k_BT/nm^2. These changes in bilayer elasticity, although small compared with H_B for $DC_{18:1}PC$/*n*-decane bilayers (56 kJ/(mole·nm^2) or 22.6 k_BT/nm^2; Lundbæk et al., 2010a), are sufficient to account for the changes in bilayer deformation energy (see Discussion). (Similar estimates were not possible for pioglitazone and ciglitazone because the lifetime changes were small, and the estimates were susceptible to even minor experimental noise.

TABLE II

TZD induced changes in the free energy of dimerization of gA channels

TZD	$\Delta G_{tot\ gA\text{-}(13)}^{M\to D}$	SD	$\Delta G_{tot\ AgA(15)}^{M\to D}$	SD
1 μM troglitazone	−5.0	0.60	−4.0	0.8
30 μM rosiglitazone	−5.0	0.2	−4.0	0.9
10 μM pioglitazone	−4.6	1.2	−4.2	1.3
6 μM ciglitazone	1.7	1.7	−0.6	2.4

Results in kJ/mole, n = 2–4.

The ciglitazone-induced changes in τ, however, are a result of changes in bilayer elasticity, as evident from the larger changes in τ of the gA^-(13) channels, relative to the AgA(15) channels [Figs. 5 D, S5 D, and 6], and from the larger changes in τ of the AgA(15) channels in the thicker $DC_{20:1}PC$/*n*-decane bilayers [Fig. S6], as compared with the $DC_{18:1}PC$/*n*-decane bilayers [Fig. 5 D].)

Effects of cholesterol. We tested the most and least potent bilayer-modifying TZDs (troglitazone and pioglitazone) in cholesterol-containing bilayers. Cholesterol increases the bilayer elastic moduli (Evans and Needham, 1987; Evans and Rawicz, 1990; Needham and Nunn, 1990), meaning that the bilayers are more difficult to deform (Evans and Needham, 1987; Lundbæk et al., 1996). Similarly to what was found with polyunsaturated fatty acids (Bruno et al., 2007), troglitazone has greater effects on gA lifetime (Fig. S8 A) and appearance frequency (Fig. S8 B) in cholesterol-containing bilayers. Pioglitazone, which had no effect on τ in cholesterol-free bilayers, changed neither τ (Fig. S7 A), *f* (Fig. S7 B), nor $\Delta G_{bil}^{M\to D}$ (Fig. S7 C).

TZD effects in hydrocarbon-free bilayers. Planar bilayers used in the electrophysiological experiments contain decane. We also did experiments in hydrocarbon-free lipid vesicles, using a fluorescence-based assay for gA channel activity (Ingólfsson and Andersen, 2010). To monitor gA channel activity, ANTS-loaded large unilamellar vesicles are mixed with Tl^+, and the time course of fluorescence quenching is recorded (Fig. S8). The resulting quenching rate provides a measure of the time-averaged number of channels in the vesicles. Except for ciglitazone, the TZDs increased the quenching rates, with troglitazone being the most potent and pioglitazone the least (Fig. 7). Ciglitazone reduced the quenching rate, indicating that the (hydrophobic mismatch–dependent) reduction in channel appearance rate (Fig. 5 H) dominates over the increase in channel

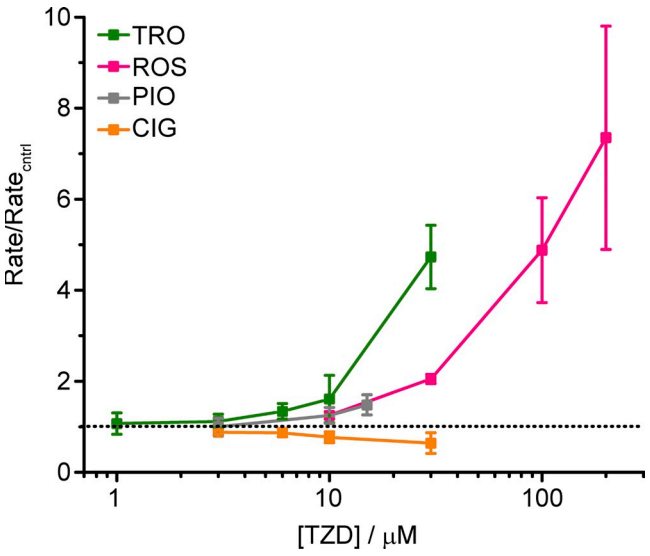

Figure 7. Effects of TZDs on the rate of Tl^+-induced fluorescence quenching of ANTS encapsulated in large unilamellar vesicles. ANTS-containing $DC_{22:1}PC$ vesicles doped with gA were incubated for 10 min at 25°C with troglitazone (TRO, olive squares), rosiglitazone (ROS, pink squares), pioglitazone (PIO, gray squares), or ciglitazone (CIG, orange squares) before mixing with Tl^+ using a stopped-flow spectrofluorometer. The quench rate was determined by fitting a stretched exponential to the time course of fluorescence quenching and determining the rate at 2 ms. Quench rates in the presence of the TZD are normalized to control quench rate in the absence of TZDs (n = 2–10).

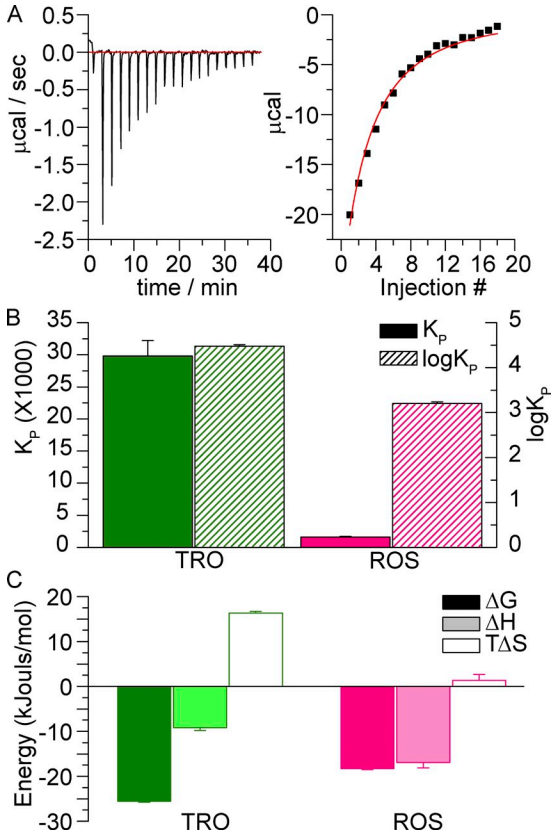

Figure 8. Partitioning of troglitazone and rosiglitazone into lipid bilayers. (A) Heat production as a function of time as 2-μl aliquots of a 10-mM lipid vesicle solution is injected into 200 μM of rosiglitazone solution. Each injection results in a peak in the energy versus time signal (left); the area under the peak corresponds to the enthalpy of partitioning for that injection, which is plotted as a function of the injection number (■, right panel). The solid line denotes the fit of Eq. 7 to the results to determine the partition coefficient ($K_P^{W\to L}$) and the molar enthalpy of partitioning ($\Delta H_P^{W\to L}$). (The partitioning of troglitazone was tested by titrating 30 μM troglitazone with 3 mM lipid.) (B) The partition coefficient $K_P^{W\to L}$ (solid fill bars) and $\log K_P^{W\to L}$ (hatched fill bars) for troglitazone (olive) and rosiglitazone (pink). (C) $\Delta G_P^{W\to L}$ (dark filled bars), $\Delta H_P^{W\to L}$ (light filled bars), and $T\Delta S_P^{W\to L}$ (open bars) for troglitazone (TRO, pink) and rosiglitazone (ROS, pink). n = 3; error bars are plotted.

lifetime (Fig. 5 D), leading to an overall reduction in channel activity.

The relative increases in quenching rates follow the pattern observed in the single-channel experiments (Fig. 5), and the effective concentration ranges and the order of TZD potencies are the same in both systems. The three TZDs that increase channel activity increase the quench rate; ciglitazone, which decreases channel activity, decreases the quench rate. The effects of the TZDs in hydrocarbon-free membranes are comparable to their effects in the presence of decane.

TZD partitioning into lipid bilayers. Hydrophobicity, as measured by octanol–water partitioning (logP: partitioning of only a single, usually the neutral, species; or $\log D_{7.4}$: distribution of all species present at pH 7.4), varies among the TZDs, with troglitazone and ciglitazone being the most hydrophobic, followed by pioglitazone and rosiglitazone (legend to Fig. 1). LogP (or logD) thus provides a good estimate for the partition coefficient of neutral, but not charged, solutes into lipid bilayers (Escher and Schwarzenbach, 1996). For the weakly acidic TZDs, pK_a values of ∼6.4 (Giaginis et al., 2007), the different electrostatic properties of the bilayer interface and the octanol–water phase may cause clogP (and $\log D_{7.4}$) to be poor predictors of TZD partitioning into bilayers. (pK_a of the adsorbed TZDs is likely to be higher than the bulk pK_a [cf. Peitzsch and McLaughlin, 1993], and it is unclear what fraction of the TZDs at the bilayer–solution interface is charged.) We therefore examined the interactions of TZDs with lipid bilayers using isothermal titration calorimetry (Heerklotz and Seelig, 2000).

Only rosiglitazone and troglitazone produced sufficient heats of partitioning to determine $K_P^{W\to L}$. Fig. 8 A (left) shows the titration of 200 µM rosiglitazone with 10-mM lipid vesicles (the lipid vesicle dilution enthalpy is negligible [Fig. S9] and is not considered in the data analysis).

Plotting the enthalpy per injection versus the injection number (Fig. 8 A, right) and fitting Eq. 7 to the results allows for determining $K_P^{W\to L}$ (Fig. 8 B) and $\Delta H_P^{W\to L}$, $\Delta G_P^{W\to L}$, and $T\cdot\Delta S_P^{W\to L}$ (Fig. 8 C). Log $K_P^{W\to L}$ for both rosiglitazone (3.2) and troglitazone (4.5) were higher than the corresponding $\log D_{7.4}$ (legend to Fig. 1). The thermodynamic profile for the partitioning of troglitazone differed from that for rosiglitazone, with entropy dominating the former and enthalpy the latter, which could reflect different locations within the bilayer–solution interface.

TZD effects on Na_V on cell membranes

Voltage-dependent inhibition of Na^+ currents (I_{Na}). As noted above (Table I), the TZDs modulate a variety of membrane proteins. We explored this question further using endogenous TTX-sensitive sodium currents in ND7/23 cells. We have previously found that amphiphiles that alter gA channel function (increase f and τ) also alter the function of voltage-dependent calcium and sodium channels (Na_V) (Lundbæk et al., 1996, 2004, 2005). We therefore explored whether the TZDs also alter Na_V function, and we compare their relative potencies on Na_V and on gA channels as probes of changes in bilayer properties.

The TZDs produce a prepulse-dependent inhibition of peak I_{Na} (Fig. 9 A). This was examined further using an alternating pulse protocol (Lundbæk et al., 2004). See the bottom of Fig. 9, with conditioning prepulses to either −130 mV (V_0) or to a voltage at which about half the channels are in the fast-inactivated state ($V_{1/2} \approx -68 \pm 2$; see Fig. 9 B). After ∼5 min of stable baseline recordings using this protocol, the TZDs were applied. The peak I_{Na} during the test pulse was strongly reduced by 6 µM troglitazone (Tables III and S2), and the inhibition was stronger after a prepulse potential to $V_{1/2}$ than to V_0 (Fig. 9).

The inhibition was fully reversible when tested from V_0, but only partially so when tested from $V_{1/2}$ (Tables III and S2). Similar complete and partial reversibility

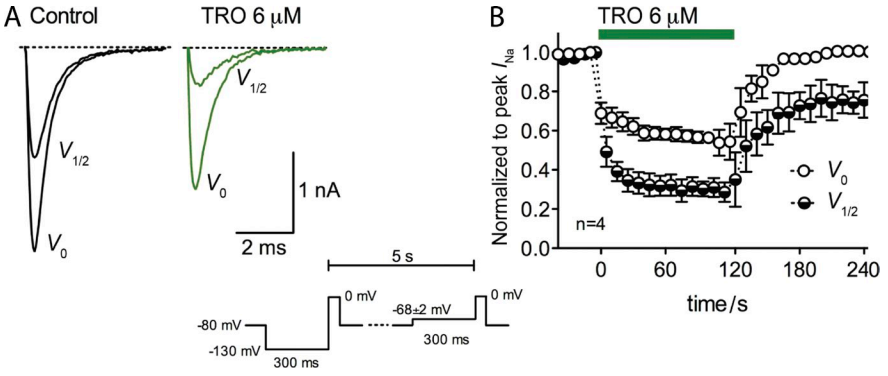

Figure 9. Effect of troglitazone on Na_V. (A) Macroscopic Na^+ current traces elicited with a pulse to 0 mV in control (left panel, black traces) or in the presence of 6 µM troglitazone (TRO, right panel, olive traces) after a 300-ms prepulse to either −130 mV (V_0) or to a voltage at which approximately half of the channels are in the fast-inactivated state ($V_{1/2}$ of ≈68 mV). (B) Time course of wash-in and washout of 6 µM troglitazone (TRO) during an alternating pulse protocol applied every 5 s in which the prepulse potential was either V_0 or $V_{1/2}$ (see inset for pulse protocol). The currents are normalized to the peak I_{Na} in control. Troglitazone inhibits peak I_{Na}, and the inhibition is larger after a prepulse to $V_{1/2}$. The inhibition was fully reversible after washout (2 min) when tested after a prepulse to V_0 mV; the inhibition was only partially reversible when tested after a prepulse to $V_{1/2}$ ($n = 4$).

after prepulses to V_0 or $V_{1/2}$, respectively, was observed with rosiglitazone. In contrast, the I_{Na} inhibition by ciglitazone (at 6 µM) did not reverse for either conditioning pulse after washout times that were effective for troglitazone and rosiglitazone (2 min). Pioglitazone caused minimal current inhibition (at 10 µM). Fig. 10 compares inhibition of peak I_{Na} at the highest concentrations tested, with 6 µM troglitazone being the strongest and 10 µM pioglitazone being the weakest inhibitor.

As in the bilayer experiments, ciglitazone increased the capacitance in the whole cell experiments (6 µM ciglitazone increased the capacitance ~15%, which was partially reversible after washout; not depicted); the other TZDs had no discernible effect. The ciglitazone-induced capacitance increase most likely reflects intramembrane transfer, as has been observed with other hydrophobic anions (Fernández et al., 1983).

Effects of TZDs on Na_V inactivation. The steady-state inactivation (h_∞ in the Hodgkin and Huxley, 1952, model) curve was determined using a double-pulse protocol. All the TZDs produced a hyperpolarizing shift in $V_{1/2}$ (Fig. 10 and Tables III and S3). The largest shift was seen with 6 µM troglitazone (−13.2 ± 4.1 mV, n = 6, and $P < 0.001$ vs. control), followed by 200 µM rosiglitazone (−5.4 ± 1.5 mV, n = 3, and $P < 0.05$), 6 µM ciglitazone (−3.0 ± 1.9 mV, n = 4, and $P < 0.05$), and 10 µM pioglitazone (−2.3 ± 0.4 mV, n = 4, and $P < 0.01$). Timed control experiment, done with the control buffer solution, showed no shift in $V_{1/2}$ during perfusion of the drug-free "sham drug" solution and subsequent "sham wash" (Table III and Fig. S10).

To determine whether the TZD-induced changes in Na_V function could be related to the TZD-induced changes in gA channel function, we compared changes in $V_{1/2}$ (Fig. 11 B) to relative changes in gramicidin lifetime (Fig. 11 A) for each compound, as plotted in Fig. 11 C. The divergent $V_{1/2}$–[TZD] relations (Fig. 11, A and B) can be superimposed when using the TZD-induced changes in τ as a measure for the TZD-induced changes in bilayer properties. The $V_{1/2}$–[TZD] relations can be superimposed on the $V_{1/2}$–[amphiphile] relations observed previously in studies on capsaicin and various detergents (Lundbæk et al., 2005). The amphiphile-induced changes in Na_V (and gA channel) function do not appear to result from direct channel–amphiphile interactions but from altered channel–bilayer interactions.

DISCUSSION

TZDs alter gramicidin channel function at concentrations where they alter the function of many membrane proteins, including Na_V. The changes in Na_V function

TABLE III

The effect of TZDs on peak I_{Na} and Na_V inactivation

Experimental condition	Inhibition of peak I_{Na}									
	Prepulse to V_0		Prepulse to $V_{1/2}$			$V_{1/2}$ of Na_V inactivation				
	norm I_{Na}	SD	norm I_{Na}	SD	n	$V_{1/2}$ (mV)	SD	n	$\Delta V_{1/2}$	SD
Control	1.00	#	1.00	#	7	−68	2.3	6	−13	4.1
6 µM troglitazone	0.62[a]	0.12	0.36[a]	0.13	7	−81[a]	4.8	6		
Wash	0.97	0.05	0.79	0.08	7	−73[a]	1.8	4		
Control	1.00	#	1.00	#	3	−70	1.9	3	−5	1.5
200 µM rosiglitazone	0.74[b]	0.04	0.60[b]	0.04	3	−76[c]	1.5	3		
Wash	0.97	0.01	0.76	0.03	3	−76	2.1	3		
Control	1.00	#	1.00	#	4	−72	2.8	4	−2	0.4
10 µM pioglitazone	0.97	0.02	0.91[b]	0.01	4	−74[b]	2.5	4		
Wash	1.01	0.05	0.89	0.11	4	−75[c]	3.0	3		
Control	1.00	#	1.00	#	7	−69	1.5	4	−3	1.9
6 µM ciglitazone	0.74[a]	0.03	0.72[a]	0.11	7	−72[c]	0.4	4		
Wash	0.77	0.04	0.76	0.16	7	−71	1.3	4		
Control	n/a		n/a			−68	2.5	5	0.3	0.8
Sham drug	n/a		n/a			−68	2.4	5		
Sham wash	n/a		n/a			−68	3.2	5		

The TZD effects on peak I_{Na} after prepulses to −130 mV (V_0) or to a voltage at which approximately half the channels are in the fast-inactivated state ($V_{1/2}$). The currents were measured after 1-min perfusion of the drug. Fractional peak I_{Na} was normalized to the control value. Right column of the table shows the effects of TZDs on steady-state inactivation (or Na^+ channel availability h_∞ in the Hodgkin and Huxley, 1952, model). $V_{1/2}$ values were determined in control after 1-min perfusion of the drug and after 2-min washout of the drug. All TZDs significantly shifted $V_{1/2}$ toward hyperpolarized potentials. Stimulation protocols as described in detail in Materials and methods and can also be seen in Fig. 10.

[a]$P < 0.001$ versus control by paired two-tailed Student's t test.

[b]$P < 0.01$ versus control by paired two-tailed Student's t test.

[c]$P < 0.05$ versus control by paired two-tailed Student's t test.

correlate with the changes in gA channel function, following the pattern observed previously for other amphiphiles (Lundbæk et al., 2005; Fig. 11), suggesting that the TZDs (and the other amphiphiles) alter the function of both channels through a common mechanism. Given that the only common feature of gA and Na_V channels is that they are embedded in lipid bilayers, the most likely common mechanism is that the TZDs adsorb to lipid bilayers to alter their properties. As we discuss below, the changes in gA and Na_V channel function occur at TZD concentrations that are similar to (for ciglitazone, pioglitazone, and troglitazone) or somewhat higher than (rosiglitazone) the plasma concentrations in patients (or animals) treated with TZDs.

We first discuss the concentrations at which the TZDs alter lipid bilayer properties; TZDs bind to plasma proteins and partition between the electrolyte and bilayer, and the free concentrations will be less than the nominal concentrations. We next consider the changes in gA channel function, as reporters of changes in bilayer properties. We then consider the possible confounding effects of *n*-decane in the planar bilayer experiments. Next, we discuss the changes in Na_V channel function and the relationship between the changes in Na_V and gA channel function. Finally, we consider how changes in lipid bilayer properties may constitute a general mechanism for the off-target effects of hydrophobic/amphiphilic drugs, including the TZDs.

At what concentrations do the TZDs alter lipid bilayer properties?

The TZDs are hydrophobic, with octanol–water partition coefficients, expressed as clogP or $logD_{7.4}$, between 2.8 and 2.6 (for rosiglitazone) and 5.7 and 4.6 (ciglitazone; legend to Fig. 1). Thus, they are likely to partition into bilayers and bind to proteins, and the free

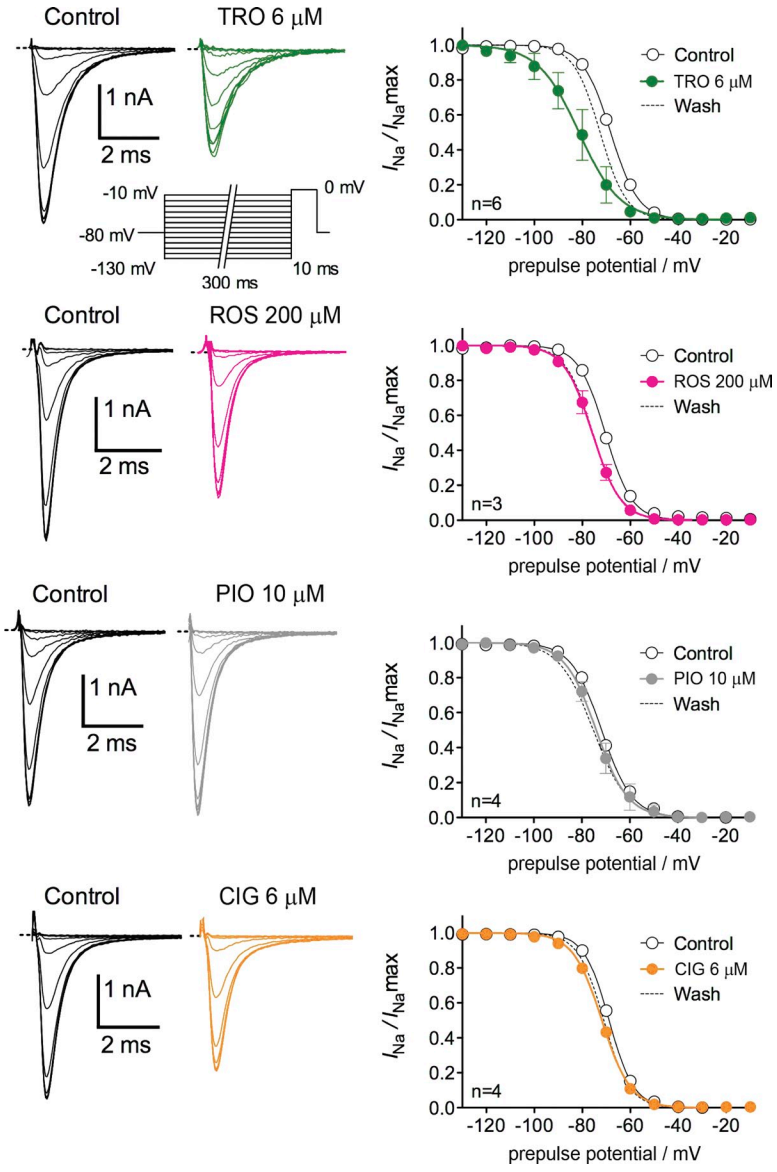

Figure 10. The effect of TZDs on Na_V steady-state fast inactivation. The left panels show families of Na^+ current traces recorded using a 10-ms test pulse to 0 mV after 300-ms conditioning prepulses to potentials ranging from −130 to −10 mV (inset shows stimulation protocol) in the absence (black current traces) or presence of the drug (colored current traces). Peak I_{Na} was normalized to the maximum peak I_{Na} (elicited after a prepulse to −130 mV), plotted against the prepulse potential and fitted with a two-state Boltzmann distribution (right panels) to determine the voltage for half-maximal inactivation ($V_{1/2}$). 6 μM troglitazone (TRO, olive traces and symbols; $\Delta V_{1/2} = -13.2 \pm 4.1$ mV, $n = 6$, and $P < 0.001$ vs. control by paired two-tailed Student's *t* test), 200 μM rosiglitazone (ROS, pink traces and symbols; $\Delta V_{1/2} = -5.4 \pm 1.5$ mV, $n = 3$, and $P < 0.05$), 10 μM pioglitazone (PIO, gray traces and symbols; $\Delta V_{1/2} = -2.3 \pm 0.4$ mV, $n = 4$, and $P < 0.05$), and 6 μM ciglitazone (CIG, orange traces and symbols; $\Delta V_{1/2} = -3.0 \pm 1.9$ mV, $n = 4$, and $P < 0.05$).

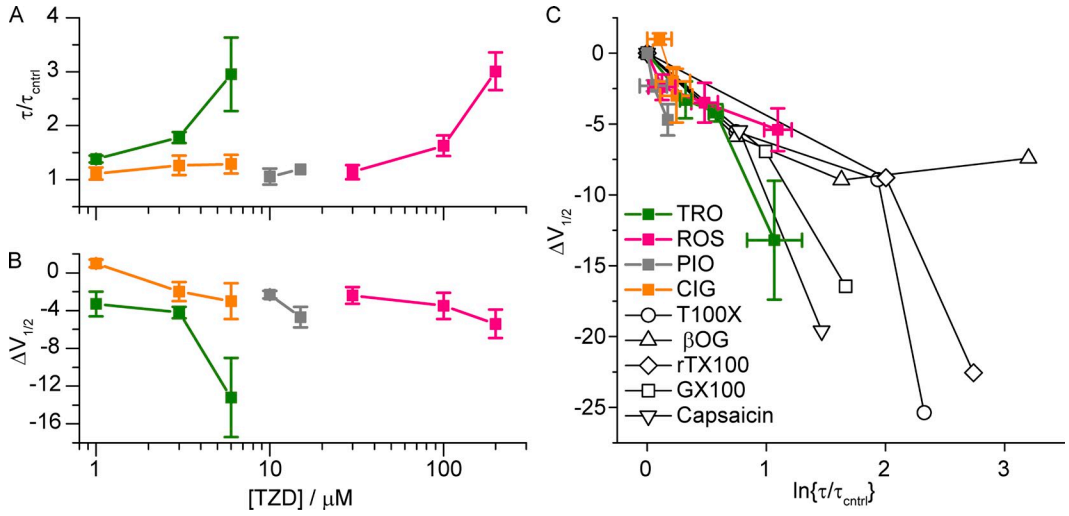

Figure 11. Comparison of the TZDs' effects on Na_V and gA channels. (A) The concentration dependence of the TZD-induced changes in AgA(15) single-channel lifetimes (τ/τ_{cntrl}; n = 1–7; mean ± SD). (In the experiment with 15 μM pioglitazone, there was visible precipitation.) (B) The concentration-dependent shifts in $V_{1/2}$ for inactivation. (n = 2–6; mean ± SD). (C) The TZD-induced shifts in $V_{1/2}$ versus the natural logarithm of relative changes in AgA(15) single-channel lifetimes. The $\Delta V_{1/2}$ versus $\ln(\tau/\tau_{cntrl})$ relations for troglitazone (TRO, olive squares), rosiglitazone (ROS, pink squares), pioglitazone (PIO, gray squares), and ciglitazone (CIG, orange squares) are very similar among the TZDs, as well as to the relations observed previously for other bilayer modifiers: Triton X-100 (TX100), β-octyl glucoside (βOG), reduced Triton X-100 (rTX100), Genapol X-100 (GX100), and capsaicin (Lundbæk et al., 2005).

drug concentration will be less than the nominal concentration (Søgaard et al., 2006; Bruno et al., 2007; Ingólfsson et al., 2007).

The TZDs are weak acids, and water–octanol partition coefficients thus may be poor predictors of TZD partitioning into bilayers (Escher and Schwarzenbach, 1996; Avdeef et al., 1998). We therefore measured their partition coefficients (K_p) into lipid bilayers using isothermal titration calorimetry. Troglitazone and rosiglitazone had sufficient partition enthalpy to allow for the determination K_p. The measured logK_ps (Fig. 8) are close to, but higher than, log$D_{7.4}$. The relationship to clogP is more complicated: for troglitazone, logK_p < clogP; for rosiglitazone, logK_p > clogP (compare Fig. 8 and legend to Fig. 1). On balance, the results suggest that one can use log$D_{7.4}$ (and clogP) to estimate the bilayer partition coefficients (see below). (The planar bilayer experiments were done using 1M NaCl, and the vesicle experiments were done using 140 mM $NaNO_3$; however, ionic strength effects on pK_a are small [cf. Harned and Owen, 1943; Rossotti and Rossoti, 1961]. Similarly, ionic strength effects on partitioning will be small because we use zwitterionic $DC_{18:1}PC$ and rather low TZD concentrations; salting-in or -out effects likewise will be small [cf. Edsall and Wyman, 1958]. We do not consider these effects further.)

Knowing the partition coefficients, we can estimate the free drug concentrations (Bruno et al., 2007; Ingólfsson et al., 2007; see Appendix). At the concentrations listed, the mole fractions (m_{TZD}) are small (Table IV), at 0.03 or less. The different mole ratio of troglitazone and rosiglitazone needed to alter bilayer properties may reflect that they localize differently in the bilayer–solution interface (as suggested by the different enthalpic and entropic contributions to the free energy of portioning). There are 10 lipids in the first shell around a gA, so there will be less than one TZD in the first shell, unless the TZDs accumulate in the perturbed bilayer adjacent to the channel (Andersen et al., 1992; Bruno et al., 2007). This is unlikely, at least in the case of ciglitazone, because the conductance changes do not depend on bilayer thickness (Fig. S11), indicating that ciglitazone does not partition preferentially into, or out of, the perturbed bilayer region (see also, Bruno et al., 2007). Although the m_{TZD}s are small, the volume-averaged TZD concentrations in the bilayer are high, ranging from 1 to 15 mM.

To compare with clinical concentrations, Table IV lists literature values for the total and free TZD concentrations in vivo and in vitro. For troglitazone and ciglitazone, the total and free plasma concentrations are similar to those in the bilayer experiments. For rosiglitazone, the concentrations in the bilayer experiments are higher than the plasma concentrations.

Changes in gA channel function and in bilayer properties

Gramicidin channels form by transbilayer dimerization of subunits in opposing bilayer leaflets (O'Connell et al., 1990), which make them suitable to probe for changes in bilayer properties (Lundbæk et al., 2010a). gA channel function, specifically the channel appearance frequency and lifetime, depends on how easy it is to deform the bilayer when the channel forms. The less energy required for bilayer deformation, the more likely it is that monomer

TABLE IV

TZD concentrations in plasma and in vitro

TZD	In vivo/clinical			Bilayer experiments			Vesicle experiments			
	Total plasma concentration	Free plasma concentration[a]	Nominal [TZD][b]	$[TZD]_a$[c]	$\{TZD\}_m$[c]	m_{TZD}[c]	$[TZD]_a$[c]	$\{TZD\}_m$[c]	m_{TZD}[c]	
	μM	*nM*	*μM*	*nM*	*moles/cm²*		*nM*	*moles/cm²*		
Troglitazone	2–6.4[d]	2–64	1	80	5×10^{-13}	2×10^{-3}	130	9×10^{-13}	4×10^{-3}	
Rosiglitazone	0.4–1.7[d]	4–17	30	18,000	6×10^{-12}	2×10^{-2}	22,100	8×10^{-13}	3×10^{-2}	
Pioglitazone	1.5–4.4[e]	36	10	5,600[f]	2×10^{-12}	10^{-2}	6,900	3×10^{-12}	10^{-2}	
Ciglitazone	37–90[g]	1,900–2,700	1	5[f]	5×10^{-13}	2×10^{-3}	9	10^{-12}	4×10^{-3}	

[a]Estimated based on protein binding.
[b][TZD] where gA channel function is altered.
[c]Estimated as described in Eqs. A7–A9.
[d]FDA (five of the links where the information can be accessed).
[e]Xue et al., 2003.
[f]Based on clogP (legend to Fig. 1).
[g]Torii et al., 1984, and Aleo et al., 2005; values for rats.

encounters will result in successful dimerization, and the smaller will be the disjoining force acting on the bilayer-spanning dimer.

Many amphiphiles, including the TZDs, alter gA channel appearance frequencies and lifetimes (see Lundbæk et al., 2010a), meaning that they alter lipid bilayer properties when they adsorb at the bilayer–solution interface. The common relation between the relative increases in τ for the gA^-(13) and AgA(15) channels caused by troglitazone, rosiglitazone, ciglitazone, and other bilayer-modifying amphiphiles (Lundbæk et al., 2010b; Fig. 6) indicates that these compounds alter gA channel lifetimes by a common mechanism that does not involve specific binding.

Ciglitazone's effects are more complex (Figs. 3 and 5). Yet, the ciglitazone-induced changes in τ follow a simple pattern (Figs. 5 D and 6). First, in $DC_{20:1}PC$ bilayers, ciglitazone causes a greater increase in τ for the shorter AgA^-(15) compared with the longer gA(17) channels (Fig. S6). Second, the increase in τ of AgA^-(15) channels in $DC_{20:1}PC$/*n*-decane bilayers is greater than the increase in AgA(15) channels in $DC_{18:1}PC$/*n*-decane bilayers (Figs. 5 D and S6), meaning that the increase in τ depends on the channel–bilayer hydrophobic mismatch. Third, ciglitazone alters τ of both AgA(15) and AgA^-(15) channels (Figs. 5 D and S6). Ciglitazone's effects on τ vary with hydrophobic mismatch, not the detailed channel structure, indicating that it alters τ through increases in bilayer elasticity.

Troglitazone, rosiglitazone, and pioglitazone increased *f*; ciglitazone decreased *f*. The changes in lifetimes and appearance frequencies caused by troglitazone and rosiglitazone follow the pattern observed for other amphiphiles (unpublished data), meaning that these molecules shift the monomer–dimer equilibrium toward the dimer and thus reduce $\Delta G_{bil}^{M\to D}$ (Table II). Pioglitazone did not change τ, indicating that it does not alter bilayer elasticity at attainable concentrations. It does, however, increase *f* for both the left-handed gA^-(13) and the right-handed gA channels, which could be because of a shift between $\beta^{6.3}$-helical and non–$\beta^{6.3}$-helical monomers (by a mechanism that does not involve direct gramicidin–pioglitazone interactions, as pioglitazone is completely inert in cholesterol-containing bilayers; Fig. S7). Ciglitazone also has complex effects. The decreases in *f* (Figs. 3 and 5 G) indicate that it alters gA channel function by a mechanism not involving changes in bilayer elasticity. Ciglitazone does not appear to interact with the $\beta^{6.3}$-helical dimers (channels); however, nor does it alter the equilibrium between single-stranded and double-stranded dimers in SEC experiments (Kapoor, R., personal communication). SEC experiments, however, are done at high gA/lipid ratios (1:20–1:100; Bañó et al., 1992), where all gA is dimeric, and do not provide information about monomers. The decreases in *f* are observed at gA/lipid mole ratios at ∼1:10^6, where gA is mostly monomeric (Durkin et al., 1990). Although bilayer-embedded gA monomers are $\beta^{6.3}$ helical at high gA/lipid ratios (He et al., 1994), maybe ciglitazone shifts the distribution among the monomers toward non–$\beta^{6.3}$-helical conformers at low gA /lipid ratios.

To check whether the changes in the gA monomer↔dimer equilibrium could be solely the result of changes in bilayer elasticity, we compare two different approaches to estimate $\Delta G_{bil}^{M\to D}$. Based on the changes in τ and using Eq. 11, 1 μM troglitazone and 30 μM rosiglitazone decrease H_B by ∼1.5 kJ/(mol·nm^2) or ∼0.6 k_BT/nm^2. Although small in relation to H_B, 56 kJ/(mol·nm^2) or 22 k_BT/nm^2 (Lundbæk et al., 2010a), these changes in H_B are sufficient to account for the measured changes in $\Delta G_{bil}^{M\to D}$. The hydrophobic mismatch-dependent contribution to $\Delta G_{bil}^{M\to D}\left(=(H_B - H_{B,cntrl})\cdot(l-d_0)^2\right)$ then can be estimated from the changes in H_B, knowing that d_0 is unchanged (see Results) (Fig. 12). This estimate for $\Delta G_{bil}^{M\to D}$ can be compared with changes in $\Delta G_{bil}^{M\to D}$ estimated using the time-averaged channel concentrations and Eq. 4 (Table II).

For AgA(15) channels, l = 2.2 nm (Table S1) and $d_0 \approx 4.0$ nm (Lundbæk et al., 2010b), and the $(H_B - H_{B,cntrl}) \cdot (l - d_0)^2$ contribution is estimated to be −4 to −7 (kJ/mol), comparable to the −4 (kJ/mol) calculated from changes in time-averaged dimer concentrations (Table II). For gA^-(13) channels, l = 1.9 nm (Table S1), and the $(H_B - H_{B,cntrl}) \cdot (l - d_0)^2$ contribution is estimated to be −5 to −9 kJ/(mol·nm^2), somewhat larger than the estimates in Table II. The effects of troglitazone and rosiglitazone can be accounted for by changes in bilayer elasticity.

Adding cholesterol to the bilayer-forming solution altered the TZD bilayer-modifying potency: troglitazone's was increased—both the lifetime and appearance rate changes were larger in the cholesterol-containing bilayers (Fig. S7); pioglitazone's was decreased—neither τ nor f was altered, suggesting that the pioglitazone-induced increases in f are not a result of specific interactions with the gramicidins. Changes in bulk membrane properties alter the TZDs' efficacy, although the direction of the changes in efficacy may vary.

The TZDs have similar effects in hydrocarbon-containing and hydrocarbon-free bilayers

TZDs alter lipid bilayer properties in both hydrocarbon-containing planar bilayers and hydrocarbon lipid vesicles (compare Figs. 5, 6, and 7). The effective concentration ranges and relative potencies were similar in planar bilayers (Figs. 5 and 6), decane-free large unilamellar vesicles (Fig. 7), and in biological membrane as reported by changes in Na_V channel function (Fig. 11).

This is not surprising. *n*-Decane–containing planar bilayers are softer than nominally hydrocarbon-free bilayers (Lundbæk and Andersen, 1999), but the ln{τ}–d_0 relations in planar bilayers are linear (Lundbæk and Andersen, 1999; Lundbæk et al., 2010a), meaning that F_{dis} is a linear function of $d_0 - l$ (cf. Eq. A5). That is, the expression for $\Delta G_{bil}^{M \to D}$ includes a term that is quadratic in $d_0 - l$ (cf. Eq. A4). We further note that the lipid intrinsic curvature usually is determined in x-ray scattering experiments on lipid–hydrocarbon systems (Turner and Gruner, 1992; Chen and Rand, 1998), and that the hydrocarbons have relatively little effect on the measured values (Chen and Rand, 1998). (*n*-Decane–containing planar bilayers are under tension [e.g., Elliott et al., 1983], whereas the lipid vesicles used in the fluorescence experiments may not be. gA channel lifetimes, however, are little affected by changes in membrane tension per se [Huang, 1986; Goulian et al., 1998], although channel function may be altered by tension-dependent changes in bilayer thickness [Goulian et al., 1998].)

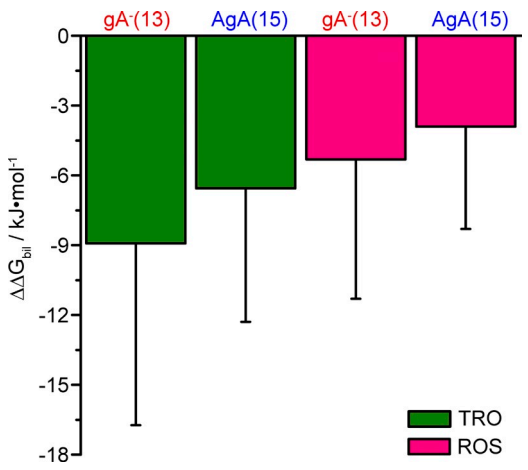

Figure 12. The troglitazone- (TRO, olive bars) or rosiglitazone- (ROS, pink bars) induced changes in the bilayer deformation energy, as determined from the changes in H_B (the hydrophobic mismatch–dependent term in Eq. A4). 1 µM troglitazone and 30 µM rosiglitazone (n = 4–6).

Changes in Na_V channel function

Previous studies have shown that troglitazone is a more potent modifier of ion channel function than the other TZDs (Table I). Few studies, however, have compared different TZDs' effects on the same system. We therefore compared the effects of the four TZDs on the activity of endogenous Na_V channels in a mammalian cell line. The TZDs inhibit peak currents and shift the $V_{1/2}$ for inactivation in the hyperpolarizing direction. Timed control experiments using a similar perfusion and pulse protocol as was used with the TZDs cause minimal changes in $V_{1/2}$ (Table III and Fig. S10). Except for ciglitazone, the inhibition is reversible when the test currents are measured after a prepulse to −130 mV, and we cannot exclude that ciglitazone interacts directly with Na_V, in addition to altering bilayer properties. When the currents are measured after a prepulse to $V_{1/2}$, the inhibition is not fully reversible, presumably reflecting that the shift in $V_{1/2}$ is not fully reversible. Maybe the TZDs accelerate the hyperpolarizing shift in $V_{1/2}$ that occurs in whole cell voltage-clamp studies (e.g., Fernandez et al., 1984; Wendt et al., 1992). In any case, the TZDs shift the equilibrium distribution between noninactivated (closed or open) and inactivated states toward the inactivated state(s). (The TZDs also alter Na_V activation [Table S4] as well as the time course of inactivation and recovery from inactivation. These changes will be the focus of a forthcoming article [unpublished data].)

Because of redistribution between the aqueous solution and the membrane and other hydrophobic compartments, the free aqueous [TZD] may differ between the bilayer system and the whole cell voltage-clamp system (Søgaard et al., 2006; Bruno, et al., 2007; Ingólfsson et al., 2007; Gingrich et al., 2009). Yet, troglitazone and rosiglitazone alter Na_V function (Fig. 11 B) at the same nominal concentrations and with the same order of potency as gA function (Fig. 11 A). When plotting the hyperpolarizing shift of $V_{1/2}$ versus the change in gA lifetime (Fig. 11 C), the relationship between the changes

in Na_V function and gA channel lifetime is remarkably similar—and not just among the TZDs but also among other bilayer-modifying compounds. This commonality suggests that these structurally diverse compounds alter both Na_V and gA channel function through a common mechanism that involves changes in bilayer properties. This does not exclude more direct drug channel interactions, for example, at the channel–bilayer boundary (Andersen, 2008), that also may alter the energetic coupling between lipid bilayers and their embedded proteins. Detergents (Deisenhofer et al., 1995) and small amphiphiles (Nury et al., 2011), for example, can bind at the protein–bilayer interface, which means that they can alter protein function by altering the energetic coupling between the bilayer and its embedded ion channels. We conclude that the TZDs alter the equilibrium between noninactivated (closed or open) and inactivated Na_v states by changing the bilayer elasticity (the bilayer deformation energy associated with the transition into the inactivated state). That is, the bilayer becomes an allosteric regulator of Na_V function.

The lipid bilayer as a mediator of off-target drug effects: implications for drug development

Our results suggest that gA channels can be used to "predict" whether amphipathic/hydrophobic molecules are likely to perturb membrane protein function, and at what concentrations. The correlation between the changes in gA channel lifetimes and the shift in the $V_{1/2}$ for Na_V inactivation is remarkable considering that Na_V channels are structurally and functionally very different from gA channels. This ability to predict changes in Na_V channel function from changes in gA function suggests that ion channel (membrane protein) function is regulated by changes in bilayer properties, including adaptations in the lipids in immediate contact with the protein, strengthening the conclusions of previous studies (Lundbæk et al., 2005; Artigas et al., 2006; Søgaard et al., 2006).

The TZDs were discovered in a search for hypolipidemic clofibrate-type compounds (Hulin et al., 1996). Ciglitazone was the first TZD to be explored for clinical use; it was discontinued during Phase II trials (Scheen, 2001). It was followed by troglitazone, rosiglitazone, and pioglitazone, the three TZDs actually marketed as insulin sensitizers. Roglitazone was later withdrawn (Scheen, 2001), and rosiglitazone is restricted in the United States (Food and Drug Administration, 2010) and suspended in Europe (European Medicines Agency, 2011).

The TZDs modify lipid bilayer properties with the order of potency, troglitazone > ciglitazone > rosiglitazone ≥ pioglitazone, which differs from their hydrophobicity (legend to Fig. 1), ciglitazone > troglitazone > pioglitazone > rosiglitazone, and their affinity for PPARγ (Table I). Ciglitazone and troglitazone are the most potent gA channel and Na_V modifiers—and the most hydrophobic. The concentrations where troglitazone alters gA channel function are similar to the clinical plasma concentrations (Table IV). Troglitazone alters the function of many membrane proteins at concentrations where it alters bilayer properties (Table I), and some of its PPARγ-independent effects, such as vasorelaxation and acute glucose uptake (Fujiwara et al., 1988; Nakamura et al., 1998; Fujiwara and Horikoshi, 2000), could arise from its bilayer-modifying effects. Troglitazone's bilayer-modifying properties also could account for its hepatotoxicity that may be a result of inhibition of hepatic bile acid transport (Snow and Moseley, 2007).

Rosiglitazone and pioglitazone, which have the least clogP and $logD_{7.4}$, are the least bilayer modifying. Pioglitazone, the least potent bilayer modifier, has less cardiovascular side effects than rosiglitazone (Graham et al., 2010; Juurlink, 2010; Nissen and Wolski, 2010). Rosiglitazone's clinical side effects, however, occur at concentrations where it has minimal bilayer-modifying effects (compare Table IV). The bilayer-modifying potency of TZDs, as expressed in changes in gA channel function, can be used to predict the likelihood and severity of side effects at the TZDs' plasma concentrations during treatment. But these drugs do, of course, also cause side effects through mechanisms unrelated to their bilayer effects.

The TZDs are part of a growing library of molecules that alter gA channel function (e.g., Lundbæk et al., 2010a). It has long been known that hydrophobic drugs have "membrane effects" (e.g., Seeman, 1972), and the bilayer-perturbing effects of hydrophobic drugs have been characterized using a variety of physicochemical probes (Seddon et al., 2009). It has proven difficult, however, to relate changes in bilayer properties, as deduced from changes in some physicochemical probes, to changes in membrane protein function, and the changes in bilayer properties may not be causally related to the changes in protein function (Spector and Yorek, 1985). Many of these difficulties can be overcome using gA channels to "sense" aggregate changes in bilayer properties and report them as changes in bilayer deformation energy (or the disjoining force acting on the channels). This is important because bilayer-spanning membrane proteins are energetically coupled to their host bilayer through hydrophobic interactions, meaning that there will be a bilayer contribution to the energetics (and kinetics) of protein conformational changes that involve the protein–bilayer boundary, which provides for mechanistic insights into hydrophobic drugs' "membrane effects."

The ability of hydrophobic drugs to alter membrane protein function correlates with their ability to alter gA channel function (Fig. 11), making it possible to explore a drug candidate's bilayer-perturbing potential early in product development (Leeson and Springthorpe, 2007; Lundbæk, 2008). It is not sufficient to focus just

on hydrophobicity ("lipophilicity" in the drug development literature), because hydrophobicity per se may not predict a compound's bilayer-modifying potential, as evident in our results and from a previous study showing that oleic acid has a higher bilayer partition coefficient than docosahexaenoic acid, yet docosahexaenoic acid is the more potent bilayer modifier (Bruno et al., 2007). A drug must be sufficiently hydrophobic to reach its target (Lipinski et al., 2001), and too high hydrophobicity is likely to be problematic because the drug may partition strongly into lipid bilayers, but increased hydrophobicity cannot be equated with increased bilayer-modifying propensity. It is important to explicitly test whether a drug lead is a bilayer modifier using probes that sense relevant (for membrane proteins) changes in bilayer properties, such as the gA channels.

APPENDIX

Energetics of lipid bilayer deformations

The bilayer deformation energy (ΔG_{def}) associated with a local bilayer thinning can be expressed as:

$$\Delta G_{def} = H_B \cdot (l - d_0)^2 + H_X \cdot (l - d_0) \cdot c_0 + H_C \cdot c_0^2, \qquad \text{(A1)}$$

where H_B, H_X, and H_C are elastic coefficients that are functions of bilayer thickness, elastic moduli, and channel radius (and include contributions from the energetic cost of redistributing the different components in multi-component membranes, including redistribution of the decane in our planar bilayers), and c_0, the intrinsic monolayer curvature (Nielsen and Andersen, 2000).

Eq. A1 can be derived from the theory of elastic bilayer deformations (Nielsen and Andersen, 2000; cf. their Eq. 17). The biquadratic structure of Eq. A1 applies more generally, however (Andersen and Koeppe, 2007). Membrane protein function is regulated by experimental maneuvers that alter bilayer thickness and intrinsic lipid curvature (Andersen and Koeppe, 2007; Tables I and II), meaning that ΔG^0_{def} can be expressed as a function of $(l - d_0)$ and c_0, and maybe other terms. Using a Taylor expansion in $(l - d_0)$ and c_0, ΔG^0_{def} becomes:

$$\begin{aligned}\Delta G^0_{def}(l - d_0, c_0) = {} & \Delta G^0_{def}(0,0) + \frac{\partial(\Delta G^0_{def})}{\partial(l - d_0)} \cdot (l - d_0) \\ & + \frac{\partial(\Delta G^0_{def})}{\partial c_0} \cdot c_0 + \frac{1}{2} \frac{\partial^2(\Delta G^0_{def})}{\partial(l - d_0)^2} \cdot (l - d_0)^2 \\ & + \frac{\partial^2(\Delta G^0_{def})}{\partial(l - d_0)\partial c_0} \cdot (d_0 - l) \cdot c_0 + \frac{1}{2} \cdot \frac{\partial^2(\Delta G^0_{def})}{\partial c_0^2} \cdot c_0^2 + \ldots,\end{aligned} \qquad \text{(A2)}$$

where the first-order terms will be zero when the bilayer can be approximated as an elastic body. (The deformation energy for small decreases in $(d_0 - l)$ should equal that for small increases of equal magnitude, with a similar argument holding for c_0.) The biquadratic form of ΔG^0_{def} in Eq. A1 thus should be valid quite generally, assuming $\Delta G^0_{def}(0,0) = 0$, with (keeping the sign convention for the H coefficients as in Lundbæk et al., 2010a, Eq. 2.6):

$$H_B = \frac{1}{2} \cdot \frac{\partial^2(\Delta G^0_{def})}{\partial(l - d_0)^2}, \; H_X = \frac{\partial^2(\Delta G^0_{def})}{\partial(l - d_0)\partial c_0}, \text{ and } H_C = -\frac{1}{2} \cdot \frac{\partial^2(\Delta G^0_{def})}{\partial c_0^2}. \qquad \text{(A3)}$$

In multi-component bilayers, the derivatives in Eqs. A2 and A3 include contributions from the redistribution of bilayer components, whether it be lipids or hydrocarbon, meaning that Eq. A1 should apply also for hydrocarbon-containing lipid bilayers, which can be approximated as elastic bodies (White and Thompson, 1973; White, 1974; Evans and Simon, 1975; Requena et al., 1975).

In Eq. A1, the $-H_C \cdot c_0^2$ term is the deformation energy associated with embedding an inclusion of length d_0 (no hydrophobic mismatch) in a bilayer with intrinsic lipid curvature c_0, because of the need for the lipids to adapt to the channel. As noted by Fattal and Ben-Shaul (1993), this expression does not include the loss of conformational entropy of the acyl chains adjacent to the channel. Using Eqs. A2 and A3, the corresponding expression becomes $\Delta G^0_{def}(0,0) + 1/2 \cdot \left(\partial^2(\Delta G^0_{def})/\partial c_0^2\right) \cdot c_0^2$, where $\Delta G^0_{def}(0,0)$ is the energetic cost of embedding an inclusion of length d_0 in a bilayer with $c_0 = 0$, including the loss of conformational entropy. Whether using Eq. A1 or Eqs. A2 and A3, the $-H_C \cdot c_0^2$ term (in Eq. A1) or $\Delta G^0_{def}(0,0) + 1/2 \cdot \left(\partial^2(\Delta G^0_{def})/\partial c_0^2\right) \cdot c_0^2$ (in Eqs. A2 and A3) drops out in the expression for $\Delta G^{M \to D}_{bil}$:

$$\Delta G^{M \to D}_{bil} = H_B \cdot (l - d_0)^2 + H_X \cdot (l - d_0) \cdot c_0. \qquad \text{(A4)}$$

The bilayer responds to the deformation by imposing a disjoining force (F_{dis}) on the channel (Andersen and Koeppe, 2007; Lundbæk et al., 2010a):

$$F_{dis} = -\frac{\partial \Delta G_{def}}{\partial(d_0 - l)} = 2 \cdot H_B \cdot (d_0 - l) - H_X \cdot c_0, \qquad \text{(A5)}$$

and changes in F_{dis}—as a result, for example, of the adsorption of TZDs at the bilayer–solution interface—will be observable as changes in τ:

$$\frac{\tau_{TZD}}{\tau_{cntrl}} = \exp\left\{-\frac{(F_{dis,TZD} - F_{dis,cntrl}) \cdot \delta}{k_B T}\right\}, \qquad \text{(A6)}$$

where δ ($\delta << d_0 - l$) is the distance the two monomers move apart to reach the transition state for channel dissociation.

F_{dis} varies as a function of the channel–bilayer hydrophobic mismatch $(l - d_0)$ and intrinsic curvature c_0, as well as the elastic moduli as expressed through the H coefficients. These contributions are separable, within the

framework provided by Eq. A3, making it possible to further explore the TZD-induced changes in bilayer properties, in particular, whether the changes in bilayer properties reflect changes in intrinsic curvature or elasticity. For example, if the TZDs cause larger relative changes in τ for the shorter than for the longer channels, the changes in F_{dis} result, at least in part, from changes in the hydrophobic mismatch-dependent term in Eq. A5. Conversely, if the TZDs cause similar relative changes in τ of the shorter and longer channels, the changes in F_{dis} result primarily from changes in the curvature-dependent term in Eq. A5.

Free drug concentrations

Let $\{TZD\}_m$ denote the [TZD] in each leaflet of the membrane (in moles/area) and $[TZD]_a$ the aqueous [TZD]:

$$\{TZD\}_m = K_p \cdot \frac{d_0}{2} \cdot [TZD]_a. \quad (A7)$$

Disregarding TZD adsorbed to the chamber, the conservation relation for the TZD becomes:

$$[TZD]_{nom} \cdot V_{aq} = [TZD]_a \cdot V_{aq} + [TZD]_m \cdot V_{lip}, \quad (A8)$$

where $[TZD]_{nom}$ is the nominal [TZD] added to the aqueous solutions, V_{aq} is the aqueous volume, and V_{lip} is the volume of the lipid-forming solution. Combining Eqs. A7 and A9:

$$\{TZD\}_m = \frac{d_0}{2} \cdot [TZD]_m = \frac{K_p \cdot [TZD]_{nom} \cdot V_{aq} \cdot d_0}{\left(V_{aq} + K_p \cdot V_{lip}\right) \cdot 2}. \quad (A9)$$

In our case, $V_{aq} = 5$ ml, $V_{lip} \approx 2$ µl, and $d_0 \approx 4$ nm (Table IV). As we could not determine K_p for pioglitazone and ciglitazone, we approximate it using clogP.

We thank Dr. Vishwanath R. Lingappa for suggesting that we explore the bilayer-modifying potential of troglitazone and other TZDs. We thank Ruchi Kapoor for the SEC experiments, and Helgi I. Ingólfsson, Ruchi Kapoor, Kevin Lum, Roger E. Koeppe II, and Jens A. Lundbæk for discussions and comments on the manuscript.

This work was supported by National Institutes of Health grants GM021342 and ARRA Supplement GM021342-35S1, GM058055, and RR015569.

Sidney A. Simon served as guest editor.

Submitted: 1 September 2010
Accepted: 1 July 2011

REFERENCES

Ahn, H.S., S.E. Kim, H.J. Jang, M.J. Kim, D.J. Rhie, S.H. Yoon, Y.H. Jo, M.S. Kim, K.W. Sung, S.Y. Kim, and S.J. Hahn. 2007. Open channel block of Kv1.3 by rosiglitazone and troglitazone: Kv1.3 as the pharmacological target for rosiglitazone. *Naunyn Schmiedebergs Arch. Pharmacol.* 374:305–309. doi:10.1007/s00210-006-0118-6

Aleo, M.D., C.M. Doshna, and K.A. Navetta. 2005. Ciglitazone-induced lenticular opacities in rats: in vivo and whole lens explant culture evaluation. *J. Pharmacol. Exp. Ther.* 312:1027–1033. doi:10.1124/jpet.104.076950

Andersen, O.S. 1983. Ion movement through gramicidin A channels. Single-channel measurements at very high potentials. *Biophys. J.* 41:119–133. doi:10.1016/S0006-3495(83)84414-2

Andersen, O.S. 2008. Perspectives on how to drug an ion channel. *J. Gen. Physiol.* 131:395–397. doi:10.1085/jgp.200810012

Andersen, O.S., and R.E. Koeppe II. 2007. Bilayer thickness and membrane protein function: an energetic perspective. *Annu. Rev. Biophys. Biomol. Struct.* 36:107–130. doi:10.1146/annurev.biophys.36.040306.132643

Andersen, O.S., D.B. Sawyer, and R.E. Koeppe II. 1992. Modulation of channel function by the host bilayer. *In* Biomembrane Structure and Function. K.R.K. Easwaran and B. Gaber, editors. Adenine Press, Schenectady, NY. 227–244.

Andersen, O.S., M.J. Bruno, H. Sun, and R.E. Koeppe II. 2007. Single-molecule methods for monitoring changes in bilayer elastic properties. *Methods Mol. Biol.* 400:543–570. doi:10.1007/978-1-59745-519-0_37

Apell, H.J., E. Bamberg, and P. Läuger. 1979. Effects of surface charge on the conductance of the gramicidin channel. *Biochim. Biophys. Acta.* 552:369–378. doi:10.1016/0005-2736(79)90181-0

Artigas, P., S.J. Al'aref, E.A. Hobart, L.F. Díaz, M. Sakaguchi, S. Straw, and O.S. Andersen. 2006. 2,3-butanedione monoxime affects cystic fibrosis transmembrane conductance regulator channel function through phosphorylation-dependent and phosphorylation-independent mechanisms: the role of bilayer material properties. *Mol. Pharmacol.* 70:2015–2026. doi:10.1124/mol.106.026070

Ashrafuzzaman, M., M.A. Lampson, D.V. Greathouse, R.E. Koeppe II, and O.S. Andersen. 2006. Manipulating lipid bilayer material properties using biologically active amphipathic molecules. *J. Phys. Condens. Matter.* 18:S1235–S1255. doi:10.1088/0953-8984/18/28/S08

Avdeef, A., K.J. Box, J.E. Comer, C. Hibbert, and K.Y. Tam. 1998. pH-metric logP 10. Determination of liposomal membrane-water partition coefficients of ionizable drugs. *Pharm. Res.* 15:209–215. doi:10.1023/A:1011954332221

Bamberg, E., and P. Läuger. 1973. Channel formation kinetics of gramicidin A in lipid bilayer membranes. *J. Membr. Biol.* 11:177–194. doi:10.1007/BF01869820

Bañó, M.C., L. Braco, and C. Abad. 1992. A semi-empirical approach for the simulation of circular dichroism spectra of gramicidin A in a model membrane. *Biophys. J.* 63:70–77. doi:10.1016/S0006-3495(92)81590-4

Berberan-Santos, M.N., E.N. Bodunov, and B. Valeur. 2005. Mathematical functions for the analysis of luminescence decays with underlying distributions 1. Kohlrausch decay function (stretched exponential). *Chem. Phys.* 315:171–182. doi:10.1016/j.chemphys.2005.04.006

Bezanilla, F., and C.M. Armstrong. 1977. Inactivation of the sodium channel. I. Sodium current experiments. *J. Gen. Physiol.* 70:549–566. doi:10.1085/jgp.70.5.549

Bruno, M.J., R.E. Koeppe II, and O.S. Andersen. 2007. Docosahexaenoic acid alters bilayer elastic properties. *Proc. Natl. Acad. Sci. USA.* 104:9638–9643. doi:10.1073/pnas.0701015104

Chen, Z., and R.P. Rand. 1998. Comparative study of the effects of several *n*-alkanes on phospholipid hexagonal phases. *Biophys. J.* 74:944–952. doi:10.1016/S0006-3495(98)74017-2

de Dios, S.T., K.M. Hannan, R.J. Dilley, M.A. Hill, and P.J. Little. 2001. Troglitazone, but not rosiglitazone, inhibits Na/H exchange activity and proliferation of macrovascular endothelial cells. *J. Diabetes Complications.* 15:120–127. doi:10.1016/S1056-8727(01)00141-6

Deisenhofer, J., O. Epp, I. Sinning, and H. Michel. 1995. Crystallographic refinement at 2.3 Å resolution and refined model of the photosynthetic reaction centre from *Rhodopseudomonas viridis*. *J. Mol. Biol.* 246:429–457. doi:10.1006/jmbi.1994.0097

Durkin, J.T., R.E. Koeppe II, and O.S. Andersen. 1990. Energetics of gramicidin hybrid channel formation as a test for structural equivalence. Side-chain substitutions in the native sequence. *J. Mol. Biol.* 211:221–234. doi:10.1016/0022-2836(90)90022-E

Edsall, J.T., and J. Wyman. 1958. Biophysical Chemistry. Volume 1. Academic Press, New York. 699 pp.

Elliott, J.R., D. Needham, J.P. Dilger, and D.A. Haydon. 1983. The effects of bilayer thickness and tension on gramicidin single-channel lifetime. *Biochim. Biophys. Acta.* 735:95–103. doi:10.1016/0005-2736(83)90264-X

Epshtein, Y., A.P. Chopra, A. Rosenhouse-Dantsker, G.B. Kowalsky, D.E. Logothetis, and I. Levitan. 2009. Identification of a C-terminus domain critical for the sensitivity of Kir2.1 to cholesterol. *Proc. Natl. Acad. Sci. USA.* 106:8055–8060. doi:10.1073/pnas.0809847106

Escher, B.I., and R.P. Schwarzenbach. 1996. Partitioning of substituted phenols in liposome-water, biomembrane-water, and octanol-water systems. *Environ. Sci. Technol.* 30:260–270. doi:10.1021/es9503084

European Medicines Agency. 2011. Avandia. http://www.ema.europa.eu/ema/index.jsp?curl=pages/medicines/human/medicines/000268/human_med_000662.jsp&murl=menus/medicines/medicines.jsp (accessed July 6, 2011).

Evans, E., and D. Needham. 1987. Physical properties of surfactant bilayer membranes: thermal transitions, elasticity, rigidity, cohesion, and colloidal interactions. *J. Phys. Chem.* 91:4219–4228. doi:10.1021/j100300a003

Evans, E., and W. Rawicz. 1990. Entropy-driven tension and bending elasticity in condensed-fluid membranes. *Phys. Rev. Lett.* 64:2094–2097. doi:10.1103/PhysRevLett.64.2094

Evans, E.A., and S. Simon. 1975. Mechanics of electrocompression of lipid bilayer membranes. *Biophys. J.* 15:850–852. doi:10.1016/S0006-3495(75)85860-7

Evans, E., W. Rawicz, and A.F. Hofmann. 1995. Lipid bilayer expansion and mechanical disruption in solutions of water-soluble bile acid. *In* Bile Acids in Gastroenterology: Basic and Clinical Advances. A.F. Hofmann, G. Paumgartner, and A. Stiehl, editors. Kluwer Academic Publishers, Dordrecht, Netherlands. 59–68.

Fattal, D.R., and A. Ben-Shaul. 1993. A molecular model for lipid-protein interaction in membranes: the role of hydrophobic mismatch. *Biophys. J.* 65:1795–1809. doi:10.1016/S0006-3495(93)81249-9

Fernández, J.M., R.E. Taylor, and F. Bezanilla. 1983. Induced capacitance in the squid giant axon. Lipophilic ion displacement currents. *J. Gen. Physiol.* 82:331–346. doi:10.1085/jgp.82.3.331

Fernandez, J.M., A.P. Fox, and S. Krasne. 1984. Membrane patches and whole-cell membranes: a comparison of electrical properties in rat clonal pituitary (GH3) cells. *J. Physiol.* 356:565–585.

Food and Drug Administration. 2010. FDA significantly restricts access to the diabetes drug Avandia. http://www.fda.gov/Drugs/DrugSafety/PostmarketDrugSafetyInformationforPatientsandProviders/ucm226956.htm (accessed July 6, 2011).

Fujiwara, T., and H. Horikoshi. 2000. Troglitazone and related compounds: therapeutic potential beyond diabetes. *Life Sci.* 67:2405–2416. doi:10.1016/S0024-3205(00)00829-8

Fujiwara, T., S. Yoshioka, T. Yoshioka, I. Ushiyama, and H. Horikoshi. 1988. Characterization of new oral antidiabetic agent CS-045. Studies in KK and ob/ob mice and Zucker fatty rats. *Diabetes.* 37:1549–1558. doi:10.2337/diabetes.37.11.1549

Funk, C., C. Ponelle, G. Scheuermann, and M. Pantze. 2001. Cholestatic potential of troglitazone as a possible factor contributing to troglitazone-induced hepatotoxicity: in vivo and in vitro interaction at the canalicular bile salt export pump (Bsep) in the rat. *Mol. Pharmacol.* 59:627–635.

Galbraith, T.P., and B.A. Wallace. 1998. Phospholipid chain length alters the equilibrium between pore and channel forms of gramicidin. *Faraday Discuss.* 111:159–164.

Giaginis, C., S. Theocharis, and A. Tsantili-Kakoulidou. 2007. A consideration of PPAR-gamma ligands with respect to lipophilicity: current trends and perspectives. *Expert Opin. Investig. Drugs.* 16:413–417. doi:10.1517/13543784.16.4.413

Gingrich, K.J., P.M. Burkat, and W.A. Roberts. 2009. Pentobarbital produces activation and block of $\alpha_{1\beta2\gamma2S}$ $GABA_A$ receptors in rapidly perfused whole cells and membrane patches: divergent results can be explained by pharmacokinetics. *J. Gen. Physiol.* 133:171–188. doi:10.1085/jgp.200810081

Goulian, M., O.N. Mesquita, D.K. Fygenson, C. Nielsen, O.S. Andersen, and A. Libchaber. 1998. Gramicidin channel kinetics under tension. *Biophys. J.* 74:328–337. doi:10.1016/S0006-3495(98)77790-2

Graham, D.J., R. Ouellet-Hellstrom, T.E. MaCurdy, F. Ali, C. Sholley, C. Worrall, and J.A. Kelman. 2010. Risk of acute myocardial infarction, stroke, heart failure, and death in elderly Medicare patients treated with rosiglitazone or pioglitazone. *JAMA.* 304:411–418. doi:10.1001/jama.2010.920

Greathouse, D.V., J.F. Hinton, K.S. Kim, and R.E. Koeppe II. 1994. Gramicidin A/short-chain phospholipid dispersions: chain length dependence of gramicidin conformation and lipid organization. *Biochemistry.* 33:4291–4299. doi:10.1021/bi00180a025

Greathouse, D.V., R.E. Koeppe II, L.L. Providence, S. Shobana, and O.S. Andersen. 1999. Design and characterization of gramicidin channels. *Methods Enzymol.* 294:525–550. doi:10.1016/S0076-6879(99)94031-4

Hamill, O.P., A. Marty, E. Neher, B. Sakmann, and F.J. Sigworth. 1981. Improved patch-clamp techniques for high-resolution current recording from cells and cell-free membrane patches. *Pflugers Arch.* 391:85–100. doi:10.1007/BF00656997

Harned, H.S., and B.B. Owen. 1943. The Physical Chemistry of Electrolytic Solutions. Reinhold Publishing Corporation, New York. 611 pp.

He, K., S.J. Ludtke, Y. Wu, H.W. Huang, O.S. Andersen, D. Greathouse, and R.E. Koeppe II. 1994. Closed state of gramicidin channel detected by X-ray in-plane scattering. *Biophys. Chem.* 49:83–89. doi:10.1016/0301-4622(93)E0085-J

Heerklotz, H., and J. Seelig. 2000. Titration calorimetry of surfactant-membrane partitioning and membrane solubilization. *Biochim. Biophys. Acta.* 1508:69–85. doi:10.1016/S0304-4157(00)00009-5

Helfrich, P., and E. Jakobsson. 1990. Calculation of deformation energies and conformations in lipid membranes containing gramicidin channels. *Biophys. J.* 57:1075–1084. doi:10.1016/S0006-3495(90)82625-4

Henke, B.R., S.G. Blanchard, M.F. Brackeen, K.K. Brown, J.E. Cobb, J.L. Collins, W.W. Harrington Jr., M.A. Hashim, E.A. Hull-Ryde, I. Kaldor, et al. 1998. N-(2-Benzoylphenyl)-L-tyrosine PPARgamma agonists. 1. Discovery of a novel series of potent antihyperglycemic and antihyperlipidemic agents. *J. Med. Chem.* 41:5020–5036. doi:10.1021/jm9804127

Hodgkin, A.L., and A.F. Huxley. 1952. A quantitative description of membrane current and its application to conduction and excitation in nerve. *J. Physiol.* 117:500–544.

Huang, H.W. 1986. Deformation free energy of bilayer membrane and its effect on gramicidin channel lifetime. *Biophys. J.* 50:1061–1070. doi:10.1016/S0006-3495(86)83550-0

Hulin, B., P.A. McCarthy, and E.M. Gibbs. 1996. The glitazone family of antidiabetic drugs. *Curr. Pharm. Des.* 2:85–102.

Hwang, T.C., R.E. Koeppe II, and O.S. Andersen. 2003. Genistein can modulate channel function by a phosphorylation-independent mechanism: importance of hydrophobic mismatch and bilayer mechanics. *Biochemistry.* 42:13646–13658. doi:10.1021/bi034887y

Ingólfsson, H.I., and O.S. Andersen. 2010. Screening for small molecules' bilayer-modifying potential using a gramicidin-based

fluorescence assay. *Assay Drug Dev. Technol.* 8:427–436. doi:10.1089/adt.2009.0250

Ingólfsson, H.I., R.E. Koeppe II, and O.S. Andersen. 2007. Curcumin is a modulator of bilayer material properties. *Biochemistry.* 46:10384–10391. doi:10.1021/bi701013n

Ingólfsson, H.I., R.L. Sanford, R. Kapoor, and O.S. Andersen. 2010. Gramicidin-based fluorescence assay; for determining small molecules potential for modifying lipid bilayer properties. *J. Vis. Exp.* 2131. doi:10.3791/2131

Juurlink, D.N. 2010. Rosiglitazone and the case for safety over certainty. *JAMA.* 304:469–471. doi:10.1001/jama.2010.954

Kapoor, R., J.H. Kim, H. Ingolfson, and O.S. Andersen. 2008. Preparation of artificial bilayers for electrophysiology experiments. *J. Vis. Exp.* 1033. doi:10.3791/1033

Katsaras, J., R.S. Prosser, R.H. Stinson, and J.H. Davis. 1992. Constant helical pitch of the gramicidin channel in phospholipid bilayers. *Biophys. J.* 61:827–830. doi:10.1016/S0006-3495(92)81888-X

Kim, B.Y., C.H. Cho, D.K. Song, K.C. Mun, S.I. Suh, S.P. Kim, D.H. Shin, B.C. Jang, T.K. Kwon, S.D. Cha, et al. 2005. Ciglitizone inhibits cell proliferation in human uterine leiomyoma via activation of store-operated Ca^{2+} channels. *Am. J. Physiol. Cell Physiol.* 288:C389–C395. doi:10.1152/ajpcell.00154.2004

Knock, G.A., S.K. Mishra, and P.I. Aaronson. 1999. Differential effects of insulin-sensitizers troglitazone and rosiglitazone on ion currents in rat vascular myocytes. *Eur. J. Pharmacol.* 368:103–109. doi:10.1016/S0014-2999(99)00020-5

Le Blanc, O.H. Jr. 1969. Tetraphenylborate conductance through lipid bilayer membranes. *Biochim. Biophys. Acta.* 193:350–360. doi:10.1016/0005-2736(69)90195-3

Lee, A.G. 2004. How lipids affect the activities of integral membrane proteins. *Biochim. Biophys. Acta.* 1666:62–87. doi:10.1016/j.bbamem.2004.05.012

Lee, K., T. Ibbotson, P.J. Richardson, and P.R. Boden. 1996. Inhibition of KATP channel activity by troglitazone in CRI-G1 insulin-secreting cells. *Eur. J. Pharmacol.* 313:163–167. doi:10.1016/0014-2999(96)00619-X

Leeson, P.D., and B. Springthorpe. 2007. The influence of drug-like concepts on decision-making in medicinal chemistry. *Nat. Rev. Drug Discov.* 6:881–890. doi:10.1038/nrd2445

Lipinski, C.A., F. Lombardo, B.W. Dominy, and P.J. Feeney. 2001. Experimental and computational approaches to estimate solubility and permeability in drug discovery and development settings. *Adv. Drug Deliv. Rev.* 46:3–26. doi:10.1016/S0169-409X(00)00129-0

Lundbæk, J.A. 2008. Lipid bilayer-mediated regulation of ion channel function by amphiphilic drugs. *J. Gen. Physiol.* 131:421–429. doi:10.1085/jgp.200709948

Lundbæk, J.A., and O.S. Andersen. 1994. Lysophospholipids modulate channel function by altering the mechanical properties of lipid bilayers. *J. Gen. Physiol.* 104:645–673. doi:10.1085/jgp.104.4.645

Lundbæk, J.A., and O.S. Andersen. 1999. Spring constants for channel-induced lipid bilayer deformations. Estimates using gramicidin channels. *Biophys. J.* 76:889–895. doi:10.1016/S0006-3495(99)77252-8

Lundbæk, J.A., P. Birn, J. Girshman, A.J. Hansen, and O.S. Andersen. 1996. Membrane stiffness and channel function. *Biochemistry.* 35:3825–3830. doi:10.1021/bi952250b

Lundbæk, J.A., P. Birn, A.J. Hansen, R. Søgaard, C. Nielsen, J. Girshman, M.J. Bruno, S.E. Tape, J. Egebjerg, D.V. Greathouse, et al. 2004. Regulation of sodium channel function by bilayer elasticity: the importance of hydrophobic coupling. Effects of Micelle-forming amphiphiles and cholesterol. *J. Gen. Physiol.* 123:599–621. doi:10.1085/jgp.200308996

Lundbæk, J.A., P. Birn, S.E. Tape, G.E. Toombes, R. Søgaard, R.E. Koeppe II, S.M. Gruner, A.J. Hansen, and O.S. Andersen. 2005. Capsaicin regulates voltage-dependent sodium channels by altering lipid bilayer elasticity. *Mol. Pharmacol.* 68:680–689.

Lundbæk, J.A., S.A. Collingwood, H.I. Ingólfsson, R. Kapoor, and O.S. Andersen. 2010a. Lipid bilayer regulation of membrane protein function: gramicidin channels as molecular force probes. *J. R. Soc. Interface.* 7:373–395. doi:10.1098/rsif.2009.0443

Lundbæk, J.A., R.E. Koeppe II, and O.S. Andersen. 2010b. Amphiphile regulation of ion channel function by changes in the bilayer spring constant. *Proc. Natl. Acad. Sci. USA.* 107:15427–15430. doi:10.1073/pnas.1007455107

Ly, H.V., and M.L. Longo. 2004. The influence of short-chain alcohols on interfacial tension, mechanical properties, area/molecule, and permeability of fluid lipid bilayers. *Biophys. J.* 87:1013–1033. doi:10.1529/biophysj.103.034280

Marsh, D. 2008. Protein modulation of lipids, and vice-versa, in membranes. *Biochim. Biophys. Acta.* 1778:1545–1575. doi:10.1016/j.bbamem.2008.01.015

Nakamura, Y., Y. Ohya, U. Onaka, K. Fujii, I. Abe, and M. Fujishima. 1998. Inhibitory action of insulin-sensitizing agents on calcium channels in smooth muscle cells from resistance arteries of guinea-pig. *Br. J. Pharmacol.* 123:675–682. doi:10.1038/sj.bjp.0701669

Needham, D., and R.S. Nunn. 1990. Elastic deformation and failure of lipid bilayer membranes containing cholesterol. *Biophys. J.* 58:997–1009. doi:10.1016/S0006-3495(90)82444-9

Nielsen, C., and O.S. Andersen. 2000. Inclusion-induced bilayer deformations: effects of monolayer equilibrium curvature. *Biophys. J.* 79:2583–2604. doi:10.1016/S0006-3495(00)76498-8

Nielsen, C., M. Goulian, and O.S. Andersen. 1998. Energetics of inclusion-induced bilayer deformations. *Biophys. J.* 74:1966–1983. doi:10.1016/S0006-3495(98)77904-4

Nissen, S.E., and K. Wolski. 2010. Rosiglitazone revisited: an updated meta-analysis of risk for myocardial infarction and cardiovascular mortality. *Arch. Intern. Med.* 170:1191–1201. doi:10.1001/archinternmed.2010.207

Nury, H., C. Van Renterghem, Y. Weng, A. Tran, M. Baaden, V. Dufresne, J.P. Changeux, J.M. Sonner, M. Delarue, and P.J. Corringer. 2011. X-ray structures of general anaesthetics bound to a pentameric ligand-gated ion channel. *Nature.* 469:428–431. doi:10.1038/nature09647

O'Connell, A.M., R.E. Koeppe II, and O.S. Andersen. 1990. Kinetics of gramicidin channel formation in lipid bilayers: transmembrane monomer association. *Science.* 250:1256–1259. doi:10.1126/science.1700867

Partenskii, M.B., and P.C. Jordan. 2002. Membrane deformation and the elastic energy of insertion: perturbation of membrane elastic constants due to peptide insertion. *J. Chem. Phys.* 117:10768–10776. doi:10.1063/1.1519840

Peitzsch, R.M., and S. McLaughlin. 1993. Binding of acylated peptides and fatty acids to phospholipid vesicles: pertinence to myristoylated proteins. *Biochemistry.* 32:10436–10443. doi:10.1021/bi00090a020

Preininger, K., H. Stingl, R. Englisch, C. Fürnsinn, J. Graf, W. Waldhäusl, and M. Roden. 1999. Acute troglitazone action in isolated perfused rat liver. *Br. J. Pharmacol.* 126:372–378. doi:10.1038/sj.bjp.0702318

Requena, J., D.A. Haydon, and S.B. Hladky. 1975. Letter: lenses and the compression of black lipid membranes by an electric field. *Biophys. J.* 15:77–81. doi:10.1016/S0006-3495(75)85793-6

Rokitskaya, T.I., Y.N. Antonenko, and E.A. Kotova. 1996. Photodynamic inactivation of gramicidin channels: a flash-photolysis study. *Biochim. Biophys. Acta.* 1275:221–226. doi:10.1016/0005-2728(96)00025-4

Rossotti, F.J., and H. Rossoti. 1961. The Determination of Stability Constants and Other Equilibrium Constants in Solution. McGraw-Hill, New York. 425 pp.

Sarafidis, P.A. 2008. Thiazolidinedione derivatives in diabetes and cardiovascular disease: an update. *Fundam. Clin. Pharmacol.* 22: 247–264. doi:10.1111/j.1472-8206.2008.00568.x

Scheen, A.J. 2001. Thiazolidinediones and liver toxicity. *Diabetes Metab.* 27:305–313.

Seddon, A.M., D. Casey, R.V. Law, A. Gee, R.H. Templer, and O. Ces. 2009. Drug interactions with lipid membranes. *Chem. Soc. Rev.* 38:2509–2519. doi:10.1039/b813853m

Seddon, J.M. 1990. Structure of the inverted hexagonal (H_{II}) phase, and non-lamellar phase transitions of lipids. *Biochim. Biophys. Acta.* 1031:1–69.

Seeman, P. 1972. The membrane actions of anesthetics and tranquilizers. *Pharmacol. Rev.* 24:583–655.

Snow, K.L., and R.H. Moseley. 2007. Effect of thiazolidinediones on bile acid transport in rat liver. *Life Sci.* 80:732–740. doi:10.1016/j.lfs.2006.11.001

Søgaard, R., T.M. Werge, C. Bertelsen, C. Lundbye, K.L. Madsen, C.H. Nielsen, and J.A. Lundbaek. 2006. $GABA_A$ receptor function is regulated by lipid bilayer elasticity. *Biochemistry.* 45:13118–13129. doi:10.1021/bi060734+

Spector, A.A., and M.A. Yorek. 1985. Membrane lipid composition and cellular function. *J. Lipid Res.* 26:1015–1035.

Stowers, M.A., A.L. van Wuijckhuijse, J.C. Marijnissen, B. Scarlett, B.L. van Baar, and C.E. Kientz. 2000. Application of matrix-assisted laser desorption/ionization to on-line aerosol time-of-flight mass spectrometry. *Rapid Commun. Mass Spectrom.* 14: 829–833. doi:10.1002/(SICI)1097-0231(20000530)14:10<829::AID-RCM951>3.0.CO;2-3

Sychev, S.V., L.I. Barsukov, and V.T. Ivanov. 1993. The double $\pi\ \pi^{5,6}$ helix of gramicidin A predominates in unsaturated lipid membranes. *Eur. Biophys. J.* 22:279–288. doi:10.1007/BF00180262

Torii, H., K. Yoshida, T. Tsukamoto, and S. Tanayama. 1984. Disposition in rats and dogs of ciglitazone, a new antidiabetic agent. *Xenobiotica.* 14:259–268. doi:10.3109/00498258409151410

Turner, D.C., and S.M. Gruner. 1992. X-ray diffraction reconstruction of the inverted hexagonal (H_{II}) phase in lipid-water systems. *Biochemistry.* 31:1340–1355. doi:10.1021/bi00120a009

Veatch, W.R., R. Mathies, M. Eisenberg, and L. Stryer. 1975. Simultaneous fluorescence and conductance studies of planar bilayer membranes containing a highly active and fluorescent analog of gramicidin A. *J. Mol. Biol.* 99:75–92. doi:10.1016/S0022-2836(75)80160-4

Wallace, B.A., W.R. Veatch, and E.R. Blout. 1981. Conformation of gramicidin A in phospholipid vesicles: circular dichroism studies of effects of ion binding, chemical modification, and lipid structure. *Biochemistry.* 20:5754–5760. doi:10.1021/bi00523a018

Wendt, D.J., C.F. Starmer, and A.O. Grant. 1992. Na channel kinetics remain stable during perforated-patch recordings. *Am. J. Physiol.* 263:C1234–C1240.

Wenk, M.R., T. Alt, A. Seelig, and J. Seelig. 1997. Octyl-beta-D-glucopyranoside partitioning into lipid bilayers: thermodynamics of binding and structural changes of the bilayer. *Biophys. J.* 72:1719–1731. doi:10.1016/S0006-3495(97)78818-0

White, S.H. 1974. Letter: comments on "electrical breakdown of bimolecular lipid membranes as an electromechanical instability". *Biophys. J.* 14:155–158. doi:10.1016/S0006-3495(74)70007-8

White, S.H., and T.E. Thompson. 1973. Capacitance, area, and thickness variations in thin lipid films. *Biochim. Biophys. Acta.* 323:7–22. doi:10.1016/0005-2736(73)90428-8

White, S.H., W.C. Wimley, A.S. Ladokhin, and K. Hristova. 1998. Protein folding in membranes: determining energetics of peptide-bilayer interactions. *Methods Enzymol.* 295:62–87. doi:10.1016/S0076-6879(98)95035-2

Xue, Y.J., K.C. Turner, J.B. Meeker, J. Pursley, M. Arnold, and S. Unger. 2003. Quantitative determination of pioglitazone in human serum by direct-injection high-performance liquid chromatography mass spectrometry and its application to a bioequivalence study. *J. Chromatogr. B Analyt. Technol. Biomed. Life Sci.* 795:215–226. doi:10.1016/S1570-0232(03)00575-0

Zhelev, D.V. 1998. Material property characteristics for lipid bilayers containing lysolipid. *Biophys. J.* 75:321–330. doi:10.1016/S0006-3495(98)77516-2

Zhou, Y., and R.M. Raphael. 2005. Effect of salicylate on the elasticity, bending stiffness, and strength of SOPC membranes. *Biophys. J.* 89:1789–1801. doi:10.1529/biophysj.104.054510

Zingsheim, H.P., and E. Neher. 1974. The equivalence of fluctuation analysis and chemical relaxation measurements: a kinetic study of ion pore formation in thin lipid membranes. *Biophys. Chem.* 2:197–207. doi:10.1016/0301-4622(74)80045-1